

MEMBRANE STRUCTURES – AN INTRODUCTION AND MANUAL FOR THE DESIGN

PROCESS OF MEMBRANE STRUCTURES

by

Niclas Hörth

Bachelor of Engineering (2015)

University of Applied Science, Karlsruhe

A thesis

presented to Ryerson University

and University of Applied Sciences Karlsruhe

in partial fulfillment of the
requirements for the degree of

Master of Engineering

in the program of
Civil Engineering

Toronto, Ontario, Canada, 2017

© Niclas Hörth, 2017

Author's Declaration

I hereby declare that I am the sole author of this thesis. This is a true copy of the thesis, including any required final revisions, as accepted by my examiners.

I authorize Ryerson University to lend this thesis to other institutions or individuals for the purpose of scholarly research.

I further authorize Ryerson University to reproduce this thesis by photocopying or by other means, in total or in part, at the request of other institutions or individuals for the purpose of scholarly research.

I understand that my thesis may be made electronically available to the public.

Title:	Membrane Structures - An Introduction and Manual for the Design- Process of Membrane Structures
Degree:	Master of Engineering
Date:	February 17 th , 2017
Universities:	University of Applied Science, Karlsruhe Ryerson University, Toronto
Name of Program:	MEng Civil Engineering
Name:	Niclas Hoerth

Abstract

Membrane structures are an frequently used architectural design element in the modern society due to their simplicity and elegance. However, these structures require often in their design process the usage of complicated numerical finite element softwares because of their non-linear behavior. Written calculations can only be used for the preliminary determination of the required pretensioning, but not for the whole design process, which includes several different loading cases. Therefore, this work with the title *Membrane Structures - An Introduction and Manual for the Design-Process of Membrane Structures* intends to develop a possible way of determining stresses in a membrane structure caused by additional loadings.

Inhalt

Membrantragwerke sind wegen ihrer Einfachheit und Eleganz ein gerne genutztes architektonisches Mittel in der Modernen Gesellschaft. Jedoch setzt der Bemessungsprozess durch die nicht-linearen Eigenschaften, häufig die Nutzung von komplizierten numerischen Finite Element Programmen voraus. Handrechnungen können nur für die Vordimensionierung der benötigten Vorspannungen durchgeführt werden, aber nicht für den ganzen Bemessungsprozess mit verschiedensten Lastfällen. Deshalb versucht diese Arbeit mit dem Titel *Membrantragwerke - Eine Einführung und Anleitung für den Bemessungsprozess von Membrantragwerken* (engl. *Membrane Structures - An Introduction and Manual for the Design-Process of Membrane Structures*) eine mögliche Herangehensweise zu entwickeln, mit der Spannungen in der Membranstruktur auch für verschiedene zusätzliche Lasten bestimmt werden können.

Contents

Author's Declaration	ii
Abstract	iii
Symbols	vi
List of Tables	viii
List of Figures	ix
1 Introduction	1
2 History of Membrane Structures	3
3 Membrane Structures	5
3.1 Type of Curvature	5
3.2 Type of Pretensioning	6
3.3 Bearing and Support	7
4 Principals of Membrane Structures	8
4.1 Load-Bearing Behavior	8
4.1.1 Mechanical Pretensioned Membranes	8
4.1.2 Pneumatic Pre-Tensioned Membranes	9
4.2 Form Finding Process	10
4.2.1 Experimental Form-Finding	11
4.2.2 Numerical Form-Finding	11
5 Components for Membrane Structures	15
5.1 Linear Load-Bearing Elements	15
5.1.1 Ropes	15
5.1.2 Webbing	16
5.2 Surface Load-Bearing Elements	17
5.3 Types of Membranes	17
5.3.1 Fabrics	17
5.3.2 Foils	18
6 Safety Concept	19
6.1 Ultimate Limit State	19
6.1.1 Loading E_d	19
6.1.2 Resistance	20
6.2 Service Limit State	22
7 Important Values	24
7.1 Steel	24
7.1.1 Solid Steel	24
7.1.2 Steel Ropes	24

7.2	Membranes	24
7.2.1	Textile Membranes	24
7.2.2	Foils	25
8	Modeling of a Preliminary Structure	26
8.1	Stitching	26
8.2	Modeling in a Special Software	26
9	Determination of Stresses with an Iterative Calculation	30
9.1	Non-Linear Approaches	30
9.2	Linear Approach	31
9.2.1	Iteration Process: Form-Finding and Calculation of Stresses	31
9.2.2	System Requirements	37
9.2.3	Soft Edges	37
9.3	Results	38
9.4	Exemplary Process	39
9.4.1	Check of the System	40
9.4.2	Iteration Process	40
10	Exemplary Calculation	48
10.1	System	48
10.2	Loadings	50
10.3	Determining Stresses	53
10.3.1	Member I	53
10.3.2	Member II	56
10.3.3	Member III	58
10.3.4	Member IV	61
10.3.5	Overview of the Stresses	64
10.4	Required Tensile Strength of the Membrane	64
10.5	Discussion of the Results	67
11	Conclusion and Prospect	69
	Bibliography	71

Symbols

Minuscule Roman symbols

α_T	Heat dilatation coefficient
γ_{DL}	Safety factors for dead loads
γ_{LL}	Safety factors for life loads
γ_m	Safety factors for membranes
γ_s	Safety factors for steel
γ_{s0}	Safety factors for steel (no buckling)
γ_{s1}	Safety factors for steel (buckling)
$\kappa_l; \kappa_t$	Force division factors load-bearing and tensioning direction for the κ -procedure
$\rho_l; \rho_t$	Force division factors load-bearing and tensioning direction for the κ -procedure

Capital Roman symbols

Δ	Elongation
σ_{Rd}	Design strength for axial forces of steel
σ_s	Characteristic strength of steel
τ_{Rd}	Design strength for shear forces of steel

Minuscule Latin symbols

$f_l; f_t$	Sags in each main-direction
n_p	Stresses caused by pretensioning
$n_{p,l}; n_{p,t}$	Pre-stresses in load-bearing and tensioning direction
$n_{q,l}; n_{q,t}$	Stresses caused by loading q in load-bearing and tensioning direction
n_t	Allowed long-time strength for 20°C for membranes
$n_{t,c}$	Characteristic tensile strength of membranes
$n_{t,d}$	Design tensile strength of membranes
$p_l; p_t$	Transformed pre-tensioning force
q	Loading
$q_l; q_t$	Loading divided in load-bearing and tensioning direction

Capital Latin symbols

A_i	Combination of reduction factors A_0 to A_3
E_d	Design value for the impact

E_s	Characteristic steel strength
$G_l; G_t$	Geometry factors in the κ -procedure
H	Total Height of the structure
L	Length
$L_l; L_t$	Lengths of load-bearing and tensioning directions
L_{rope}	Length of a edge rope
R_d	Design value of the resistance
$R_l; R_t$	Radii in load-bearing and tensioning direction
S_{sag}	Ratio of the sag in comparison to its span for edge ropes

List of Tables

6-1	Safety factors γ for different load cases	19
6-2	Safety factors γ_s for steel	21
6-3	Description of the reduction factors A_1 , A_2 and A_3	21
7-1	Tensile and shear strength of solid steel	24
7-2	Tensile strength n_k for textile membranes	25
7-3	Tensile strength f_k for foils	25
10-1	Determination of the wind loading	52
10-2	Overview of stresses	64

List of Figures

1-1	Canopy spider web	1
1-2	Assembling of airworthy animals	2
2-1	Ancient types of membrane Structures	3
2-2	Model of hanging structure (a) turned into a rod structure (b)	4
2-3	Architectural and load bearing membrane structures	4
3-1	Possibilities for curvatures of membrane structures	5
3-2	Principle of mechanical pretensioning	6
3-3	Stresses caused by pneumatic internal pressure p	7
3-4	Umbrella erected by centrifugal forces	7
3-5	Possible types of bearing of membrane structures	7
4-1	Possible membrane structures	9
4-2	System with pretensioning load p and load q from above	10
4-3	System with pretensioning load p and load q from below	10
4-4	Form finding process in the software Sofistic	12
4-5	Form-finding of a conical membrane structure with the <i>Projection Method</i>	13
4-6	Form-finding of a point-supported membrane structure	13
4-7	Form-finding of a membrane structure supported by arches	14
4-8	Form-finding of a pneumatic membrane structure	14
5-1	Assembling of wire ropes	15
5-2	Different types of ropes	16
5-3	Different usages of ropes for membrane structures	16
5-4	Load-Bearing behavior of membranes	17
5-5	Weaving types	18
6-1	Description of the reduction factors A_0 , A_1 , A_2 and A_3	21
6-2	Reduction factors A_1 , A_2 and A_3	22
6-3	Development of pools at the edges in a FE-model in <i>Dlubal RFEM</i>	23
8-1	Stitching process for modeling a structure into <i>Dlubal RFEM</i>	26
8-2	Stitching process for modeling a complex structure into <i>Dlubal RFEM</i>	27
8-3	Modeling of a simple structure in Rhino and its input in a static software	27
8-4	Modeling of a complex structure in Rhino and its input in a static software . . .	28
8-5	Procedure of the import and export of a generated model	29
9-1	Exemplary alysoid for different load cases	33
9-2	Geometry of edge ropes	37
9-3	Calculation of the force N_{rope}	38
9-4	Results of n_l of the iteration process for various loadings q	39

9-5	Results of n_t of the iteration process for various loadings q	39
9-6	Results of $n_{p,l}$ and $n_{p,t}$ for the chosen range of loadings	46
9-7	Close up view of the results of the iteration process (orange) and the static software <i>Dlubal RFEM</i> (grey)	47
10-1	Visualization of the roofing of the bus station	48
10-2	Cross section of the roofing on the narrow end	48
10-3	Cross section of the roofing on the broad end	49
10-4	Overview of the further investigated parts of the structure	49
10-5	Modeling of Member I	49
10-6	Modeling of Member II	49
10-7	Modeling of Member III	50
10-8	Modeling of Member IV	50
10-9	Breakdown of the roof area	51
10-10	Measurements of Member I	53
10-11	Measurements of Member II	56
10-12	Measurements of Member III	58
10-13	Measurements of Member IV	61
10-14	Actual Height of Member IV	62

1 Introduction

"We try to realize what nature is by studying the self-formation process of large real objects that can be explained by neither physics nor chemistry alone. We are seeking the principles of formation."

- Frei Otto (1925 - 2015) -

The general idea of light-weight structures is to put only the material there, where it is really required and has a purpose, everything else can be left out. Exactly this is the kind of functional evolution of forms, shapes and structures, can we find everywhere around us in nature. All different types of living creatures or plants are specialized in their appearance or physical abilities exactly for their surrounding environment.

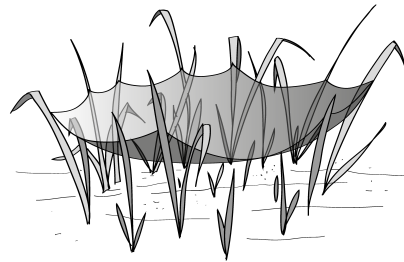
As the opening quotation of Frei Otto indicates, he was trying to analyze the capacity of many natural appearances. He specialized in the topic of light-weight structures. However this work will solely concentrate on the special topic of membrane structures.

Trying to apply the ideas of nature on membrane structures, one small structure comes practically naturally to mind: spiderwebs.

Especially the web the of the canopy spider can be seen as a natural example of the simple shaping of membrane structures (cf. Figure 1-1) as it is spread horizontally in between blades of grass with developed high- and low-points and flexible edges around the surface. However, due to the constant force of gravity and lack of additional vertical support, the web sags after a while and is endangered to break with attacking wind or rain.



(a) Canopy spider web [1]



(b) Illustration of a canopy spider web [2]

Figure 1-1: Canopy spider web

Therefore another idea of the nature has to be consulted: for example the wings of flightable animals, a bat, a bird or even a Pterodactyl. The skin of the wings has to be stabilized to ensure the continuous and controllable flow of air and wind around them. This stabilization is gained by the mechanical tensioning of the skin with the help of the skeleton and muscles (see Figure

1-2). Applying this idea of pretensioning onto a canopy spider web, could stabilize it vertically for impacts like rain and wind.

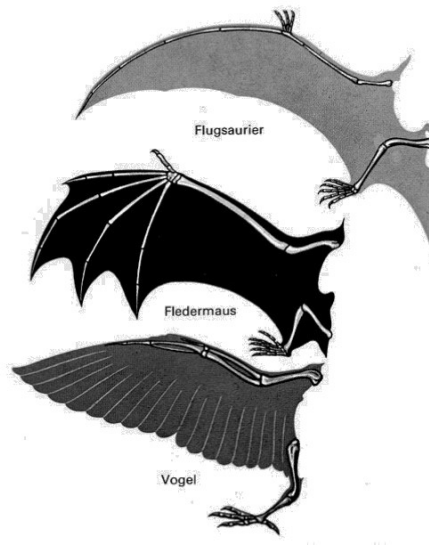


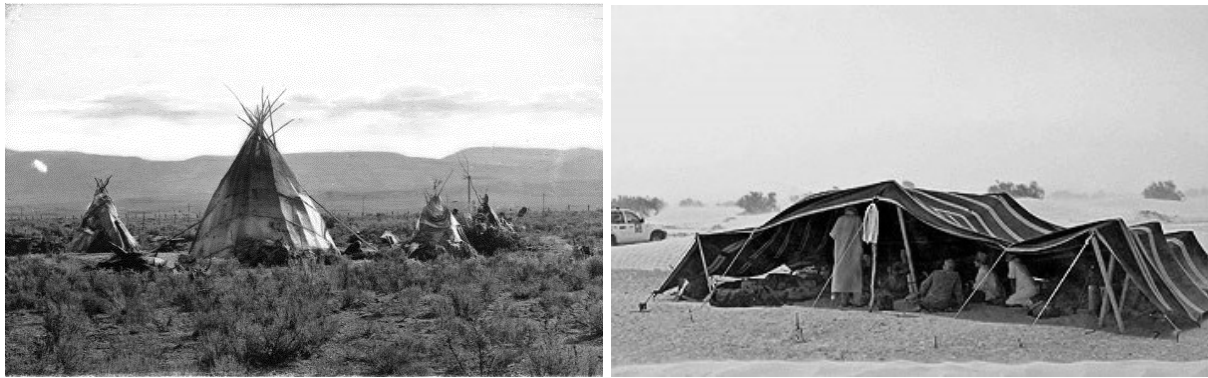
Figure 1-2: Assembling of airworthy animals (from top to bottom: Pterodactyl, bat, bird) [3, p.17]

This leads to the general idea of membrane structures, where the ensemble acting of both, the shape and pretensioning are an essential part of modern membrane structures and of their design process. However, more detailed approaches are discussed in the following work.

2 History of Membrane Structures

This chapter will give a short introduction of the history of membrane structures and then will move on to the distinctions and divisions of the structure and its influence on the static system.

For about 2000 years the construction with ropes and membranes was limited to temporal constructions like tents or shading structures (see Figure 2-1). These buildings had short spans due to the imitated quality of the used materials, which were e.g. sticks and leather. With the development of wrought iron in the 19th century those light-weight structures found their way into architecture and midway through the 20th century the spans were getting large with the usage of ropes. [4, p.V]



(a) Tipi tent of Native Americans [5]

(b) Beduin shading structure [6]

Figure 2-1: Ancient types of membrane Structures

One of the pioneers that developed the type of structures known today was Frei Otto. He recognized the possibility to describe the shape of membranes by only high- and low-points with a freely span in between by studying parts of nature like for example a spiderweb. Which is a perfect natural example of a three-dimensional rope-net. [4, p.V]

He also developed complicated shells by the simple usage of hanging structures. Following the rule of the principals of ropes, which can only bear tensile stresses, the idea is to flip them by 180°, so that the pure tensile stresses will become pure pressure, without any shear stresses (cf. Figure 2-2).

Today membrane structures are often used for architectural purposes, like the shadowing structure in front of the *Bundeskanzleramt* in Berlin (cf. Figure 2-3 (a)) or serve as surface load-bearing elements, like the roof of stadiums (cf. Figure 2-3 (b)).

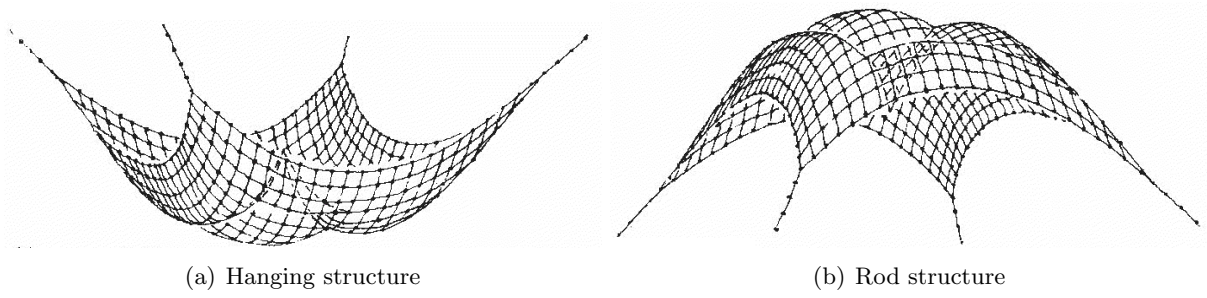
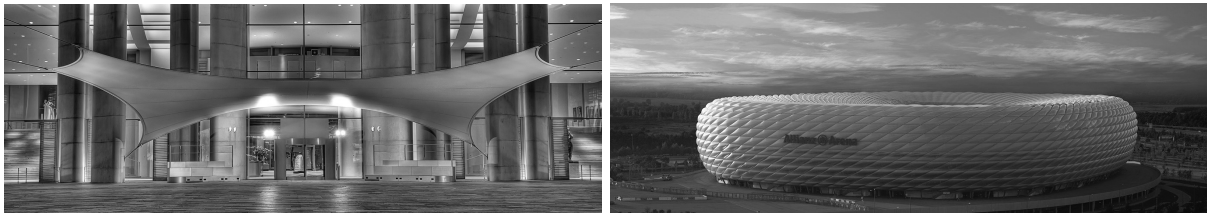


Figure 2-2: Model of hanging structure (a) turned into a rod structure (b) [7]



(a) Architectural membrane in front of the *Bundeskanzleramt* in Berlin [8] (b) Load bearing facade made out of membranes for the Allianz Arena in Munich [9]

Figure 2-3: Architectural and load bearing membrane structures

The development of materials and the ability to influence their properties makes membranes nowadays a widespread alternative, that gains attention. The sole problem is the not standardized design process. There are several different approaches, each different in their assumptions and acceptance level.

3 Membrane Structures

Membrane structures can be distinguished in their appearance and therefore in their design process. Those distinctions are:

- type of curvature,
- type of pretensioning,
- bearing and support,
- formation of the membranes - single or multiple-layer construction,
- three-dimensional arrangement of the membrane

and will be discussed further in this following chapter. [10, p.6-8]

3.1 Type of Curvature

Figure 3-1 shows all four different possibilities of curvature of membrane structures.

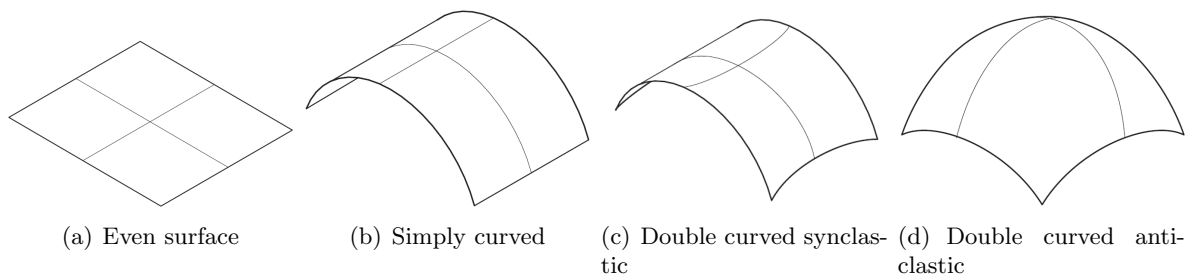


Figure 3-1: Possibilities for curvatures of membrane structures [10, p.6]

- (a) shows an even flat surface, which cannot be realized perfectly, as the membrane will always have a slight slope. However, the smaller the slope, the higher the necessary axial forces at the boundaries and therefore the stresses inside the membrane itself.
- (b) shows a simply curved membrane. Those kind of membrane structures are only usable for design purposes, as they are unable to carry any load reliably.
- (c) shows a double curved synclastic curvature, which is often used in pneumatic supported membrane structures. The form of both (c) and (d) will be given by the equilibrium of forces inside of the membrane and not by the designer.
- (d) shows a double curved anticlastic curvature. This is the only type, that can securely and reliably serve as a load bearing element in a structure without to add inner pressure to the membrane.

3.2 Type of Pretensioning

There are three different types of pretensioning of membranes.

- mechanical pretensioning
- pneumatic pretensioning
- centrifugal force

Mechanical Pretensioning

Mechanical pretensioning is induced into the membrane by producing it smaller then necessary and then pull it in the correct shape. By pulling the membrane, it is exposed to tension and will elongate following Hooke's Law expressed by Equation 3.1) slightly alternated for membrane structures. A more detailed examination using Poisson's numbers can be neglected as the change in volume due to elongation are minimal for membranes.

$$\Delta L = \frac{n_{membrane}}{E} \cdot L \quad (3.1)$$

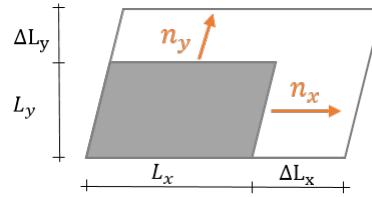


Figure 3-2: Principle of mechanical pretensioning

Pneumatic Pretensioning

The other type of pretensioning a membrane uses of internal pressure inside of the structure. The internal pressure presses the membrane surface until it is in its final shape. An approximate calculation can be made with the usage of Barlow's formula (see Equations 3.2, 3.3 and Figure 3-3).

Fun fact: The effect described by Barlow's formula is the cause, why sausages when heated always tear up lengthways, as the stress there is twice as high then diagonally.

$$n_{circumference} = \frac{p \cdot R}{t} \quad (3.2)$$

$$n_{axial} = \frac{p \cdot R}{2 \cdot t} \quad (3.3)$$

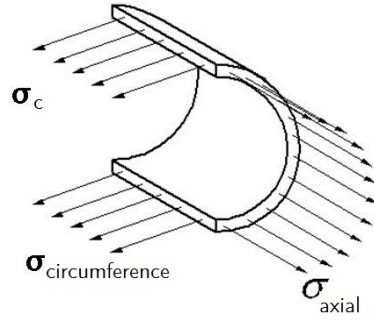


Figure 3-3: Stresses caused by pneumatic internal pressure p [11]

Centrifugal Forces

It is also possible to tighten membranes by using centrifugal forces. Then the membrane is mounted on a rotation plate, which erects by turning the membrane through the arising centrifugal forces. It is a highly complex process depending on the span, weight of material and revolutions per minute. *Werner Sobek* examined and developed this type of membrane structures in 2003 (cf. Figure 3-4). [12]



Figure 3-4: Umbrella erected by centrifugal forces [12]

3.3 Bearing and Support

Membrane surfaces need to be beared constantly along their edges. Those bearings can be formed like shown in Figure 3-5, where (a) shows a linear bearing at the bottom edges and a punctuate support at the top, (b) has linear bearings at its edges, made out of cables (also called soft bearings) and (c) has similar to (a) linear bearings at its bottom, however those bearings work also as a surface support, as this particular structure has to be sealed at the edges.

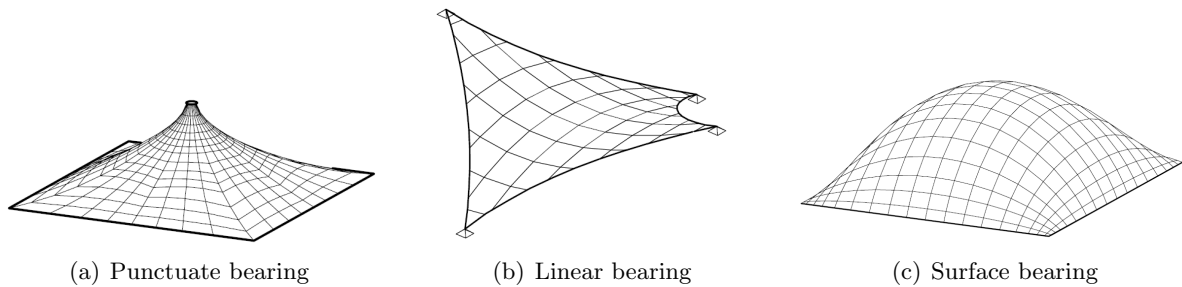


Figure 3-5: Possible types of bearing of membrane structures [10, p.7]

4 Principals of Membrane Structures

This chapter will give a short overview of the general principals of membrane structures. The load-bearing behavior, the form-finding process, some information about the membrane material and the development of the final and correct cut.

4.1 Load-Bearing Behavior

Membranes have no pressure- or bending-resistance, a negligible shear capacity and high deflections. Therefore, membranes can only bear tension as they react to pressure with instant buckling or fall into folds. Only in surface effective forces produce a constant loading over the thin membrane thickness which means an optimal exploitation of the material.

Plane membranes cause relatively high internal as well as external forces (see chapter 3.1), therefore the only stable variation are double curved membranes. The form of these double curved membranes depends on the type pretensioning. There are two different types of pretensioning, the mechanic and pneumatic pretensioning. [10, p.9]

4.1 Mechanical Pretensioned Membranes

The mechanical pretensioning is induced at the edges of the membrane. The membrane will adjust in an equilibrium of internal and external forces as well as deflection, this process is called form-finding (see chapter 4.2). When the edges are not on the same level a double curved surface arises. This means, that on each point on the surface the main curvature are on different sides of the tangent plane. This can be expressed in the so called *Gaussian Curvature*. [10, p.10]

Gaussian Curvature

Each point is defined by its curvature and therefore its radius of curvature:

$$k_1 = \frac{1}{R_1} \qquad k_2 = \frac{1}{R_2}$$

The product of the curvature in both main directions is called the *Gaussian Curvature*:

$$k = k_1 \cdot k_2 = \frac{1}{R_1} \cdot \frac{1}{R_2}$$

Is the *Gaussian Curvature* positive the double bended surface is called synclastic and if it is negative anticlastic (see Figure 4-1).

To consider the anisotropic properties of the membrane materials, it is possible to assume a different pre-stressing force in each main direction. This assumption can also be used, to alternate the form of the membrane, as a higher stress in one direction will pull the whole form in its

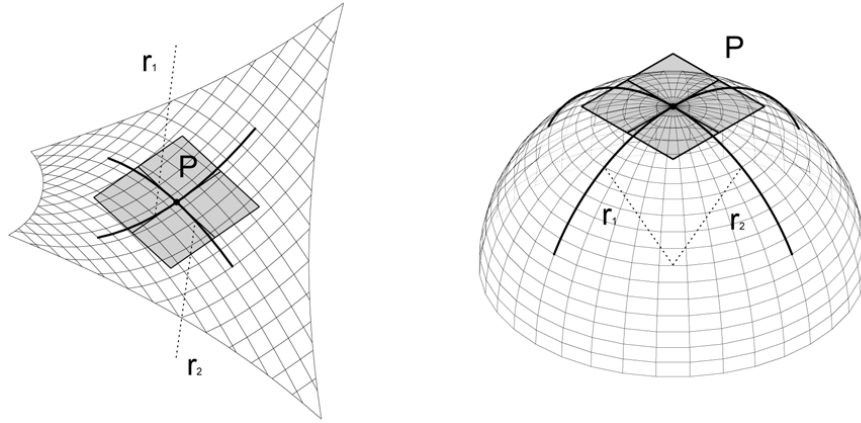


Figure 4-1: Possible membrane structures - left: anticlastic surface; right: synclastic surface [10, p.11]

direction. [10, p.10]

A large curvature produces always lower stresses for the same loading then a smaller one. This means, as previously mentioned, that a nearly plane surface always goes with high stresses as well as the danger of water and snow bags. [10, p.10]

Load-bearing behavior of double bended membranes

Figure 4-2 and 4-3 are showing the nature of membranes, whereas the load-bearing direction changes its position and faces always the loading q (orange lines) on the simple example of a four-point supported membrane (see Figure 4-1 left). In both figures the pretensioning force p and the additional loading q are applied in their individual direction of action. Whereas the load q will always increase the stresses in the load-bearing direction, it will decrease the stresses in tensioning direction simultaneously.

Hence, the tensioning direction will fail when the loading q becomes greater then the pretensioning force p . Therefore, to ensure the stability of the system, the pretensioning force p is one of the significant values and has to be chosen appropriately. Also the stresses in load-bearing direction are not allowed to overcome the maximum tensile strength of the membrane (see Chapter 6.1.2). [10, p.11]

4.1 Pneumatic Pre-Tensioned Membranes

The pneumatic pretensioning is considered to be an area-loading. The difference of pressure between a closed-up medium, such as gases or a fluid and the surrounding medium pretensions the membrane. In the state of equilibrium the tension in the membrane and the over- or under-pressure are equal. The structure usually has a positive *Gaussian Curvature* which means a synclastic form (see Figure 4-1). [10, p.12]

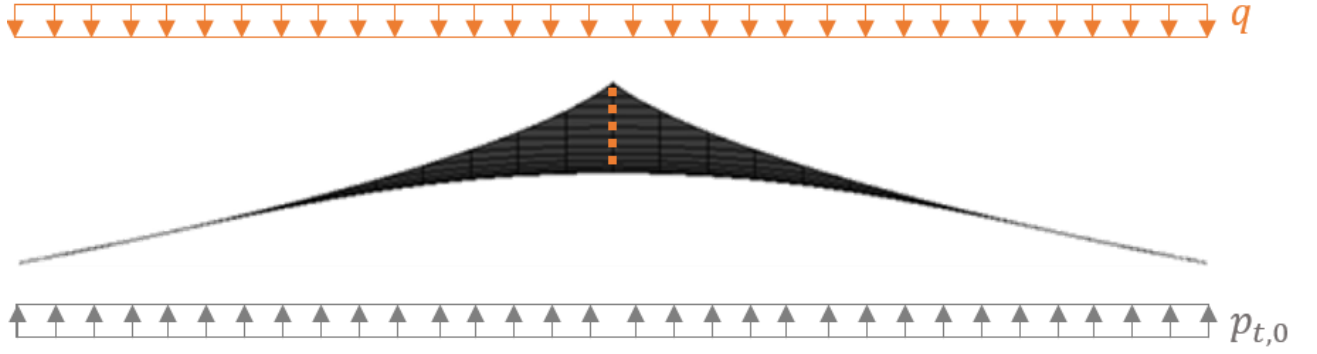


Figure 4-2: System with pretensioning load p and load q from above

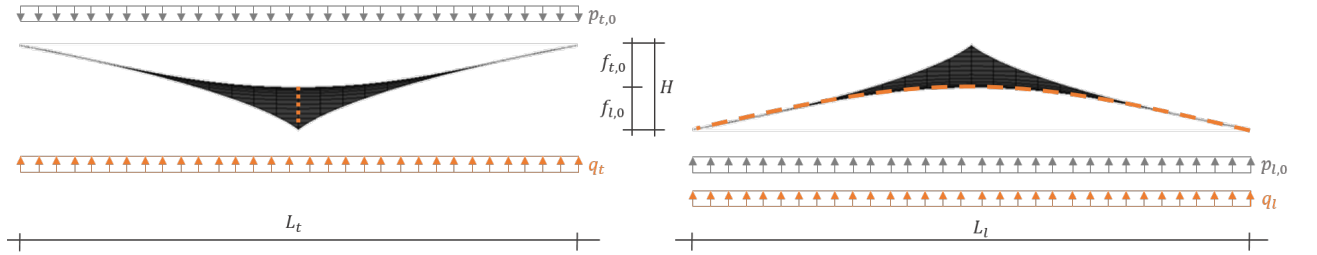


Figure 4-3: System with pretensioning load p and load q from below

4.2 Form Finding Process

As previously mentioned, the form of pretensioned membranes is a result of a equilibrium of the internal and external forces. All form but few exceptions cannot be incorporated by simple geometric shapes, as they would lead folds, local overloading and inhomogeneous states of tension inside the membrane. The aim of the form finding process is to find this equilibrium between the shape and forces.[10, p.12]

Minimal Surface

The shape of the membrane surface is a mathematical problem and is called a minimal surface, which is defined as the surface in a space with the local minimal surface area. In a mechanical and structural point of view, a minimal surface is the shape a membrane takes in the case, that each main direction has consistent stresses. However, there is not only one definite minimal surface, as it can change with different amount of pretensioning in each axis, also the loading will have an influence on the shape. There are several experimental approaches to find and map a minimal surface.

Minimal surfaces are of limited usage in the case of membrane structures. The applied materials often have anisotropic properties also the seams between the individual membrane lines will cause differences in the stiffness of the membrane in each direction. [10, p.13]

4.2 Experimental Form-Finding

For a long time experimental form-finding was the only possibility to determine the shape of double bended membranes. There are three different models which differ in their development of the membrane structure:

- Design models
- Measurement models
- Special models

Design Models

Even today design models are essential for the design process of membrane structures and are usually build out of fabric, wire or soap skin. Those models are a fast, simple and cheap method to present first ideas and the spatial effect. Therefore are these models most of the time quite simple and rough in their dimensions and serve only as a basis for the ongoing design process.

For example, the usage of a soap skin model is where a soap skin is put into the three dimensional outlines of the designed structure. The characteristics of soap skin is, that it will always shape in its most stable way and that is always a minimal surface. Hence, the shape the soap skin will take in this experiment is the minimal surface for its isotopic pretensioned form. This approach was developed at the Institute for light-weight structures at the University Stuttgart and was conducted by Frei Otto (see Chapter 2). [10, p.13]

Measurement Models

These precise built models are used to define the final shape of a membrane structure and are the basics for the execution of the structure as well as the design process and final cutting of the membrane. [10, p.13]

Special Models

Special models can be used to investigate specific areas of the structure. They find application for example in wind tunnel or movement testings or the detailed depiction of boundary elements that can be further examined with these kind of models. [10, p.13]

4.2 Numerical Form-Finding

The method of numerical form-finding increased its importance with the fast development of computing power. It is easy and quick to implement the numerical model in a software and change its properties as often as necessary to identify the best shape. Also the possibilities to change other characteristics such as the stresses in the membrane or vary boundary elements

to get the optimal result. In short, the now available changes to optimize a structure are the foundation for the modern design process of membrane structures.

An example is shown in Figure 4-4, where the shape was found with an finite element software called *Sofistic*. The initial geometry is shown in the left Figure and the final on the right, the Figure in the middle shows a staging post in the calculation process.

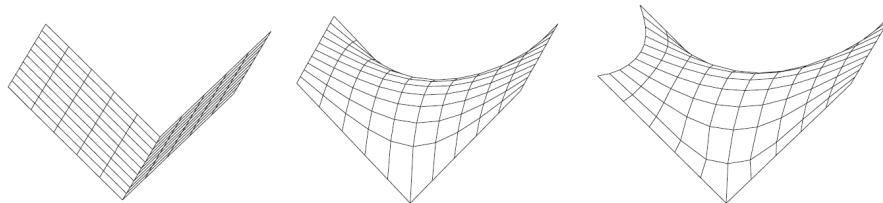


Figure 4-4: Form finding process in the software Sofistic [10, p.35]

There are several different methods to get a suitable solution. All of them are approximation procedures, where the wanted shape is described by an idealized model made out of small elements (e.g. rods, triangles or quadrilaterals, etc.). [10, p.15]

One of the key features of a numerical form-finding process is the fact, that "there is a direct correlation between the loading pre-stress and the shape of membrane structures" [13, p.3] and also that the process is independent of any material properties. However, as the methods are almost always an iteration process, it is important to change the settings to an sufficient amount of iteration steps to ensure the accuracy of the final results.

The subsequently utilized finite element static software *Dlubal RFEM* uses two different methods, which are both based on the form-finding method *Updated Reference Strategy* short URS published by K.U. Bletzinger and E. Ramm in 1999:

- Projection Method
- Tension Method

Projection Method

The *Projection Method* is used for the calculation of high conical shapes (see Figure 4-5). It uses also the certain equilibrium condition, which claims, that it is possible to determine stresses tangential of the direction of all adjacent points on the basis of a certain equilibrium condition, when the loading was defined in a radial direction. The *Projection Method* projects the prestresses on the XY plane. If the membrane inclination against the global XY plane equals zero, the stress in the membrane corresponds to the preset values. If it "is unequal to zero, the prestress in the fall line (loading) direction increases whereas the prestress in the contour line (tensioning) direction decreases." [13, p.3-4] It "allows the prestress equilibrium to be preserved in the direction of the global axes X and Y. In the form-finding process, the program then seeks such a layout of the membrane structure in space that provides for the equilibrium prestress in the direction of the global axis Z as well." [13, p.4]

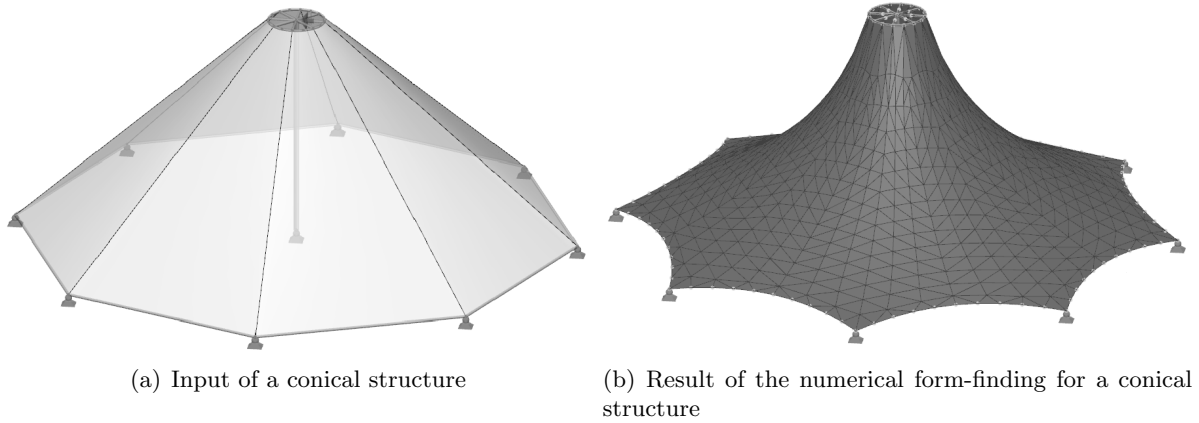


Figure 4-5: Form-finding of a conical membrane structure with the *Projection Method* [13, p.23-24]

Tension Method

Whereas the *Projection Method* is applicable on conic structures, the *Tension Method* is used for membranes supported by points and arches as well as for pneumatically stabilized structures (see Figures 4-6, 4-7 and 4-8). [13, p.4]

"The *Tension Method* is very different from the *Projection Method*: The prestress previously defined is not modified [...]. When determining the equilibrium shape, the *Tension Method* applies both values previously defined for the prestress in the warp and weft direction." [13, p.4]

It also uses the fact that "the deformations perpendicular to the membrane plane are more frequent than the deformations in the membrane plane. Once the number of iterations for using the required prestress is reached, the structure is stabilized. The resulting prestress is usually very close to the preset value." [13, p.4]

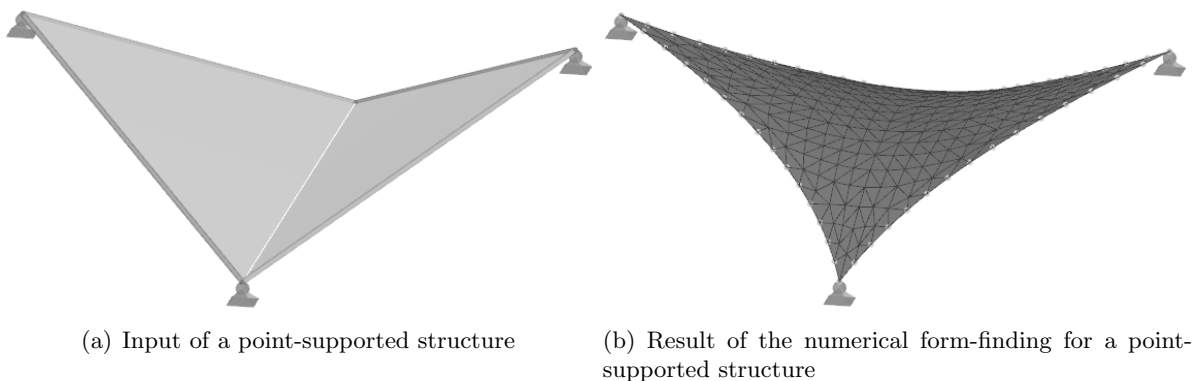
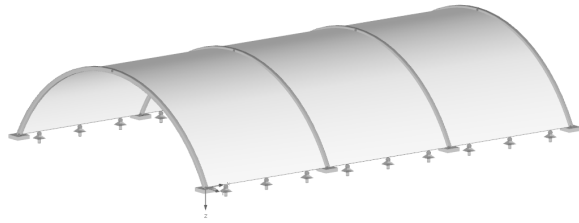
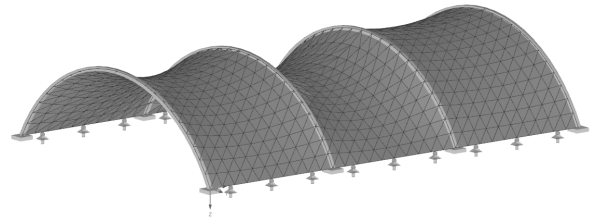


Figure 4-6: Form-finding of a point-supported membrane structure [13, p.17]

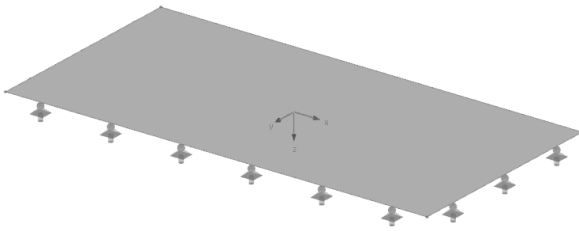


(a) Input of an arch-supported structure

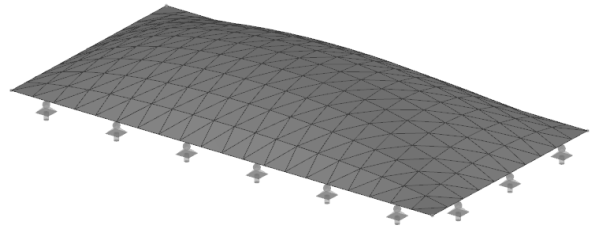


(b) Result of the numerical form-finding for an arch-supported structure

Figure 4-7: Form-finding of a membrane structure supported by arches [13, p.18]



(a) Input of a pneumatic structure



(b) Result of the numerical form-finding of a pneumatic structure

Figure 4-8: Form-finding of a pneumatic membrane structure [13, p.21-22]

5 Components for Membrane Structures

This chapter will introduce the commonly used components for membrane structures. These components can be divided into two different sections, distinguished by their load-bearing behavior [14]:

- linear load-bearing elements
- surface load-bearing elements

However, this chapter will elaborate solely on the components of actual membrane structures and not their supporting structures.

5.1 Linear Load-Bearing Elements

Linear load-bearing elements can only be used to ablate loading alongside their main axis. These elements are usually elongated and limp, such as ropes or thin steel rods. Whereas ropes can only carry tensile stresses, it is possible for rods to bear pressure, however as these rods are normally thin and long, their ability to carry pressure is limited due to buckling. Because of that it can be claimed, that linear load-bearing elements used for membrane structures are mainly used to bear tensile stresses.

5.1 Ropes

In the construction industry ropes are usually made out of steel or steel alloys and consist out of intertwined wires in a variable amount of layers. An example of an assembling is shown in Figure 5-1. Wires are twisted around another wire called strand inserts. This whole package is called a strand. Several strands surrounding one another are the actual rope.

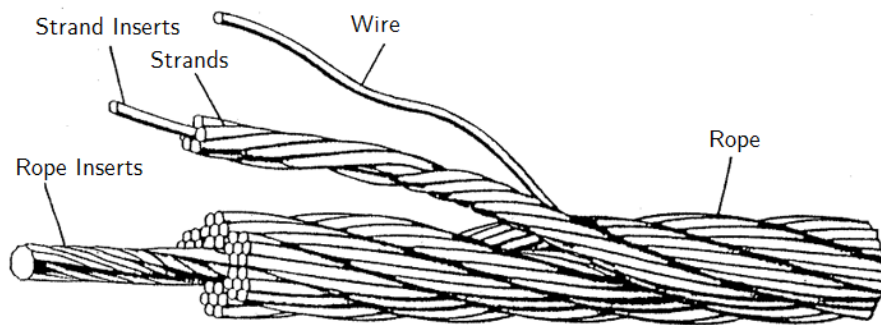


Figure 5-1: Assembling of wire ropes [15]

The thicker the final rope, the more tensile load it can carry and the less deformation it will have due to loading, the stiffness will increase though. Another distinction is made for open and fully-closed ropes which are shown in Figure 5-2.

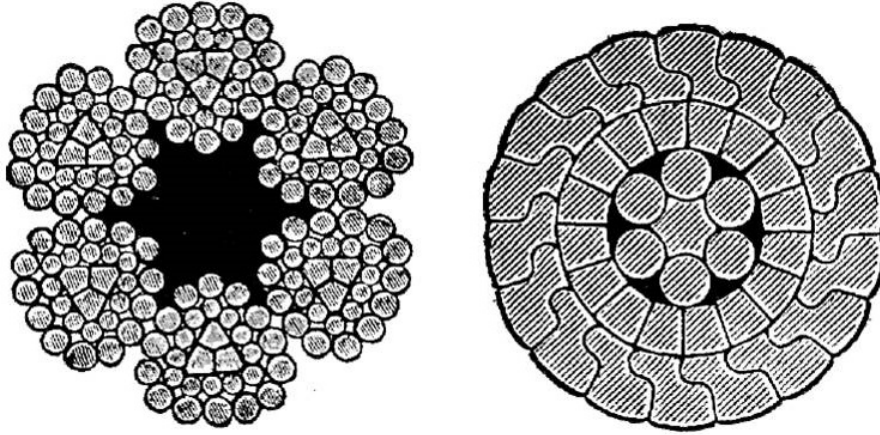


Figure 5-2: Different types of ropes (left: open rope; right: closed rope) [16]

Ropes can serve in different roles for membrane structures. For example they can be used as so called *soft edges* alongside the edge of the membrane system as shown in Figure 5-3 (a), or underneath the membrane as an additional support or to prevent the building of pools. Also ropes are often used in the supporting system of the membrane system itself, this case is shown in Figure 5-3 (b).



(a) Musical avillion in Kassel [17]



(b) Olympic stadium in Montreal [18]

Figure 5-3: Different usages of ropes for membrane structures: (a) support at the edges (*soft edges*); (b) supporting structure of the system

The material properties are given by the various manufacturers and can be inquired there if needed.

5.1 Webbing

Slender membrane cut-outs are called webbing. They are is often used to reinforce edges, as there often are the greatest stresses, due to recede material and the consequent spike in the stresses. Therefore, webbings are usually installed parallel to the edges. [14, p.24-25]

5.2 Surface Load-Bearing Elements

Surface load-bearing elements are used to cover an area and consist out of at least two main axes. Usually these elements are loaded perpendicular to their main axis, which will cause a bending moment as well as shear force, for example a ceiling. However in the case of membranes, there is no bending resistance and only a shear resistance not worth to be mentioned. Membranes ablate their internal forces by deformation. They will deform until every point in the surface is inclined enough to respond to the loading, so that it can be absorbed and converted into axial forces alongside the main axes. [14, p.26]

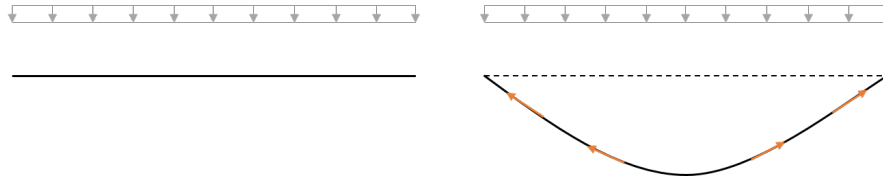


Figure 5-4: Load-Bearing behavior of membranes

Figure 5-4 above shows the deformation of membranes to allow them to carry perpendicular loads. On the left Figure is the structure undeformed and unable to carry any vertical load, therefore it deforms into the form shown on the right Figure which enables the transfer of vertical loading.

5.3 Types of Membranes

There are two different types of membranes used for structures:

- fabrics
- foils

5.3 Fabrics

Fabrics or textiles are interwoven yarns. These fabrics can be coated to alternate their properties. There are three different types of weaving, basket, twill and satin weave which are defined in the number of strings in the warp direction (cf. Figure 5-5). The type of weaving has also an immediate influence on the tensile strength in warp and weft direction. The tensile strength in twill and satin weaving is higher then in basket weaving, therefore those are preferred in membrane structures. [14, p.27-34]

Whereas uncoated membranes are usually used as sunshade and in temporary structures, coated textiles can be improved for several functions such as [4, p. 448 - 478]:

- proofness against environmental influences (e.g. water, dampness, dust and smell)
- protection of the webbing against mechanical damage

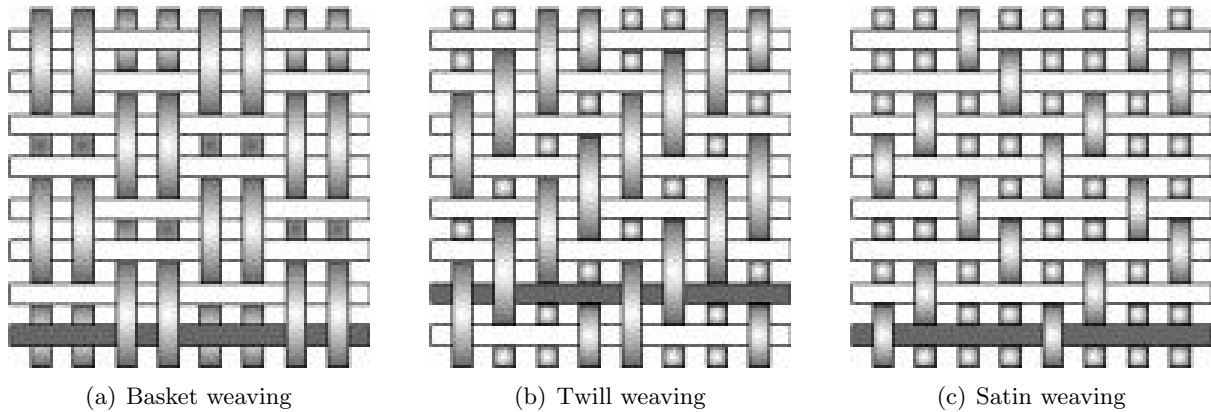


Figure 5-5: Weaving types [19]

- improving the duration of usability of the textile
- improving the protection against fire
- manufacturing of glue and weld seams
- improving the shape stability
- color
- dirt-resistant or easy to clean

5.3 Foils

The usage of foils as the membrane material is divided into temporal and permanent structures. Whereas the temporal structures are usually made out of Polyvinyl Chloride (PVC), the permanent ones are often made out of Ethylene-Tetrafluorethylene Copypolymer (ETFE) or Tetrahydrocannabivarin (THV). The thicknesses can vary from 50 to 250 μm and in some cases up to 300 μm . The low tensile strength but high shear capacity are reason for the preference of foils for pneumatic systems with short spans and pretensioned structures with low curvatures.

The type of production has an influence on the thickness of foils. The thickness of flat films depends on the rotation velocity of the take-up roll and the accuracy of the geometry. The accuracy of blow films is better then the one of flat films. [4, p.478-490]

6 Safety Concept

The idea of safety concept for membrane structures is the same used as for all common structures. The impact has to be smaller then the resistance of both the stability, also expressed as the Ultimate Limit State (ULS), and serviceability, Service Limit State (SLS). However there are some differences in the application. The exact approach is described in DIN 4134.

6.1 Ultimate Limit State

The aim of the *ULS*, is to determine the maximal loading and the resulting internal forces in the system and to make sure, that the cross-sections and materials are chosen adequately.

$$E_d \stackrel{!}{\leq} R_d \quad (6.1)$$

6.1 Loading E_d

For the determination of the design loading E_d the loading has to be multiplied with safety factors γ . They are divided into γ_{DL} for dead loads, γ_{LL} for live loads and especially for pretensioning forces γ_p . (cf. 6-2)

Table 6-1: Safety factors γ for different load cases

Impact	Live Loads γ_{DL}	Dead Loads γ_{LL}	Pretensioning γ_P
Incriminating	1.35	1.5	—
Relieve	1.00	0	—
Short-term	—	—	1.00
Long-term	—	—	1.50

Membrane structures are a special kind of structure, therefor the following combinations of characteristic stresses were taken from the code DIN 4134:1983-02 from the year 1983 [20, p.7]:

- Blizzard

$$1.00 \cdot n_{DL} + 1.10 \cdot n_p + 1.60 \cdot n_{LL} \stackrel{!}{\leq} perm.n_0$$

Where,

n_{LL} is snow or wind

n_0 is the allowed short-time strength for 20 °C

- Thunderstorm

$$1.00 \cdot n_{DL} + 1.10 \cdot n_p + 0.70 \cdot n_{LL} \stackrel{!}{\leq} perm.n_{\vartheta}$$

Where,

n_{LL} is an up-current of wind

n_{ϑ} is the allowed short-time strength for 70 °C

- Long-Term:

$$1.35 \cdot n_{DL} + 1.30 \cdot n_p \stackrel{!}{\leq} perm.n_t$$

Where,

n_t is the allowed long-time strength for 20 °C

However, these load combinations are out-of-date and a new safety concept was initiated several years ago. Therefore, following will show the more up-to-date version:

- Short-term loading for 20°C: $perm.n_{0,Rd}$

$$1.35 \cdot n_{DL} + 1.00 \cdot n_p + 1.5 \cdot n_{LL} \stackrel{!}{\leq} perm.n_0 \quad (6.2)$$

Where,

n_{LL} is snow or wind

n_0 is the allowed short-time strength for 20 °C

- Short-term loading for 70°C: $perm.n_{\vartheta,Rd}$

$$1.00 \cdot n_{DL} + 1.00 \cdot n_p + 1,5 \cdot n_{LL} \stackrel{!}{\leq} perm.n_{\vartheta} \quad (6.3)$$

Where,

n_{LL} is wind

n_{ϑ} is the allowed short-time strength for 70 °C

- Long-term pretensioning for 20°C: $perm.n_{t,Rd}$

$$1.35 \cdot n_{DL} + 1.50 \cdot n_p \stackrel{!}{\leq} perm.n_t \quad (6.4)$$

Where,

n_t is the allowed long-time strength for 20°C

6.1 Resistance

Typical materials used for membrane structures were shown in Chapter 5. However, the determination of the ultimate tensile strength is different from the calculation of the tensile strength of steel. Several impacts have influence on the strength and durability of the material.

Steel

The strength of steel is calculated by dividing the characteristic strength by the safety factor γ_s :

$$\sigma_{s,Rd} = \frac{\sigma_{s,c}}{\gamma_s} \quad (6.5)$$

Table 6-2: Safety factors γ_s for steel

γ_s	$\gamma_{s,0}$ (no buckling)	$\gamma_{s,1}$ (buckling)
	1.00	1.10

Textile Membranes

$$n_{t,d} = \frac{n_{t,c}}{\gamma_m \cdot \prod_{i=0}^3 (A_i)} = \frac{n_{t,c}}{\gamma_m \cdot A_0 \cdot A_1 \cdot A_2 \cdot A_3} \quad (6.6)$$

Figure 6-1: Description of the reduction factors A_0 , A_1 , A_2 and A_3 [21, p.151]

	Reduction factors	Description
A_0	1.00 – 1.20	multiple axis stress conditions
A_1	1.60 – 1.70	long time loading
A_2	1.10 – 1.20	reduction of strength by environment
A_3	1.10 – 1.25	increased temperature

Foils

The design value for the single-axis tensile strength $n_{t,d}$ can be calculated with Equation 6.7 and the graphs in Figure 6-3 and Table 6-2:

Table 6-3: Description of the reduction factors A_1 , A_2 and A_3 [21, p.151]

	Description
A_1	duration of loading - red: Polymethylmethacrylate (PMMA) - green: fiber-reinforced synthetic material mechanical reduced \perp - blue: fiber-reinforced synthetic material manually produced - yellow: fiber-reinforced synthetic material mechanical produced \parallel
A_2	medium class - tempered (lower line) - untempered (upper line)
A_3	service temperature

$$n_{t,Rd} = \frac{n_{t,c}}{\gamma_M \cdot \prod_{i=1}^3 (A_i)} = \frac{n_{t,c}}{\gamma_M \cdot A_1 \cdot A_2 \cdot A_3} \quad (6.7)$$

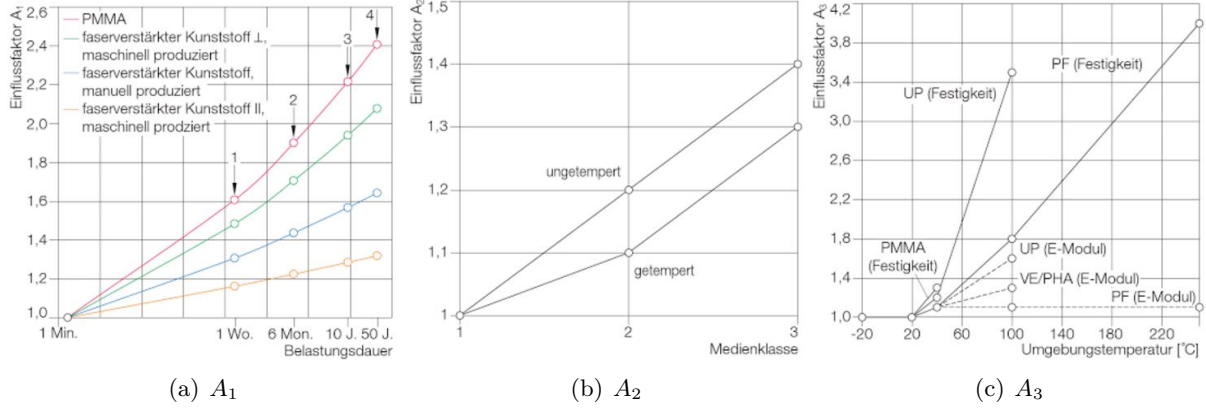


Figure 6-2: Reduction factors A_1 , A_2 and A_3 [21, p.151]

A guideline from experience is:

$$\gamma_m \cdot \prod_{i=1}^3 (A_i) = 2 \dots 4 \quad (6.8)$$

6.2 Service Limit State

The global examination of the *SLS* for membrane structures based on the shape of geometry of equilibrium of the unloaded system.

As the deformation often is the highest in edges due to loading, because there is the ratio of curvature and stress the lowest, the deformations there have to be examined properly to prevent the development of pools or other deposition, that would cause a local increase of the loading, as is shown in Figure 6-3. Each structure has to be examined individually to ensure the drainage of the surface. Hence, the SLS cannot be expressed in a equation like in other disciplines.

The Service Limit State is also defined as the usability and appearance of the membrane, which can be described with following exemplary characteristics:

- duration of the usability, influenced by e.g. different materials, coatings or weaving types
- transparency, influenced by e.g. different materials, thicknesses of the membrane or coatings
- fire resistance

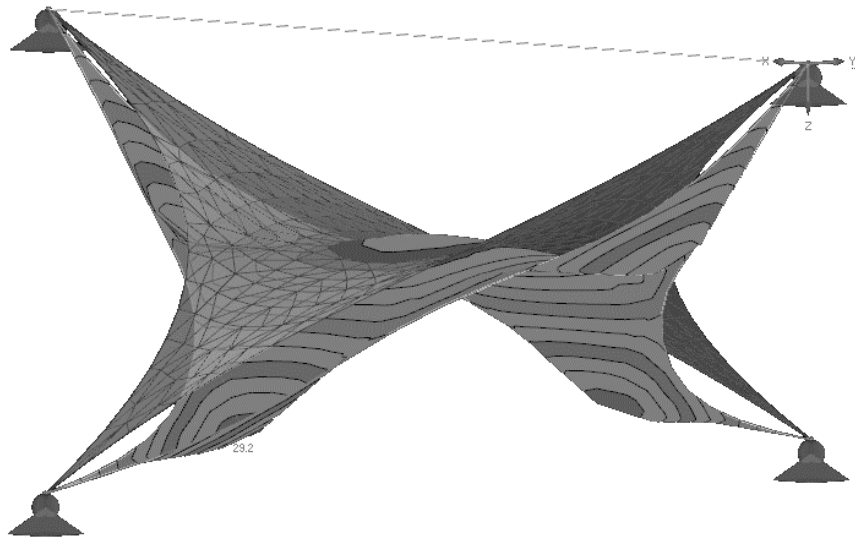


Figure 6-3: Development of pools at the edges in a FE-model in *Dlubal RFEM*

7 Important Values

The following chapter will give a few important values for the most common materials for membrane structures

7.1 Steel

Steel can be used for both solid cross-sections as a supporting structure and flexible cables for membrane structures.

7.1 Solid Steel

Table 7-1 shows the tensile and shear strength for most common used types of steel, for the each safety factor γ_m (cf. 6.1.1).

Table 7-1: Tensile and shear strength of solid steel [22]

γ_m	S235		S275		S355		S450	
	σ_{Rd}	τ_{Rd}	σ_{Rd}	τ_{Rd}	σ_{Rd}	τ_{Rd}	σ_{Rd}	τ_{Rd}
	$\left[\frac{N}{mm^2} \right]$		$\left[\frac{N}{mm^2} \right]$		$\left[\frac{N}{mm^2} \right]$		$\left[\frac{N}{mm^2} \right]$	
1.00	235	136	275	159	335	205	440	254
1.10	214	123	250	144	323	186	400	231

7.1 Steel Ropes

For information about the tensile strength of ropes it is recommended to visit the specific website of the producers, as there are many different types of ropes which all have different properties in strengths, stiffness and cross-sections.

7.2 Membranes

Membranes can be divided into two different types (cf. Chapter 5.2).

7.2 Textile Membranes

Table 7-2 shows the tensile strength and breaking elongation separated for warp and weft direction for various textile membranes. Special attention has to be placed on the possible difference in tensile strength between warp and weft direction, which can be expressed in the static software as anisotropic pretensioning.

Table 7-2: Tensile strength n_k for textile membranes [23]

Textiles	Tensile Strength warp/weft	Breaking Elongation warp/weft
	$n_c \left[\frac{kN}{m} \right]$	[%]
PVC-Polyester	60/60	15/20
	90/80	15/20
	115/100	15/25
	150/130	15/30
	195/165	20/30
PTFE-Glass Fiber	70/70	7/17
	115/115	5/12
	150/150	2/10
Silicon Glass Fiber	135/120	5/10
PTFE-Fabric	90/80	10/11

7.2 Foils

Table 7-3 shows the tensile strength and the breaking elongations for various foils. It can be seen, that the values often are given in a range. This is due to the manufacturing of the foils, where it is only possible to obey tolerances, hence the thickness and therefore the strength and breaking elongation can vary over the length of the material.

Table 7-3: Tensile strength f_k for foils [23]

Foils		Tensile Strength	Breaking Elongation
		0,25 mm $n_c \left[\frac{kN}{m} \right]$	[%]
Politetrafluoroetilen	PTFE	10 – 15	200 – 500
Perfluorethylenpropylen	FEP	5 – 6	250 – 350
Polyvinylidenfluorid	PVDF	7	500 – 600
Terpolymer	THV	7	600
Ethylen-Tetrafluorethylen	ETFE	7 – 10	300 – 425
Polyvinylfluorid	PVF	6	95 – 100
Polyethylenterephthalat	PET	50 – 60	110
Polyvinylchlorid soft	PVC-P	7	190 – 350
Polyethylen low density	PVS-LD	4 – 8	200 – 900
Thermoplastic Elastomers			
Ethyl-Vinyl-Acetat	EVA	3 – 5	600 – 900
Polyurethan	PUR	8 – 12	380 – 580

8 Modeling of a Preliminary Structure

This chapter will show two different possibilities to model a membrane structure, that can be calculated by the static software *Dlubal RFEM* with its special Add-in *RF-Formfinding* that is used for the form-finding process (see Chapter 4.2.2).

8.1 Stitching

One of the simplest types of the modeling is called stitching. It is carried out directly in the finite element static software itself and can be used for a fast way of a preliminary determination of stresses and form finding.

As the software only allows the user to type in membranes as plane surfaces the whole model has to be built by using triangular surfaces, as that is the only shape, even in a three-dimensional space.

Figure 8-1 (a) shows the process of stitching for a simple membrane structure. It is a fast and straightforward way of producing a rough preliminary design for easy membrane structures. However, the results have to be examined carefully, as the software is not able to give results on the edges of one of the previously mentioned triangular surfaces due to mathematic issues (orange lines).

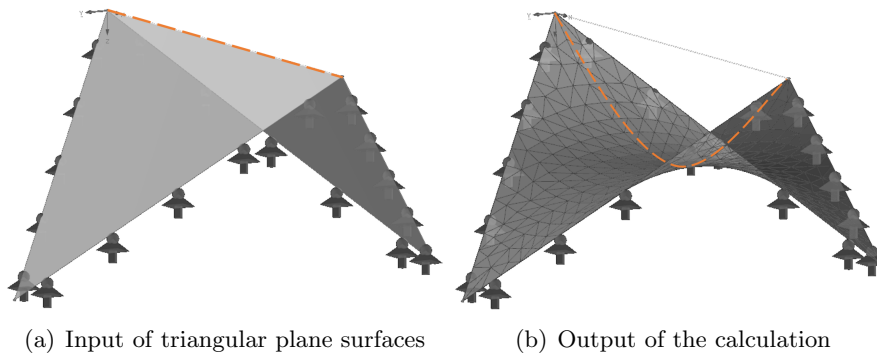


Figure 8-1: Stitching process for modeling a structure into *Dlubal RFEM*

For more complex structures like the one shown in Figure 8-2 (b), that has lots of individual triangular surfaces, the deficit of information for results can become a serious problem up to the uselessness of the whole model. Stitching also increases the expenditure of work immensely the more lines have to be connected and the more plane surfaces have to be created.

8.2 Modeling in a Special Software

There are several different professional modeling softwares that can be used to produce an integral surface in the approximate shape of the final membrane. The shape can vary in the static

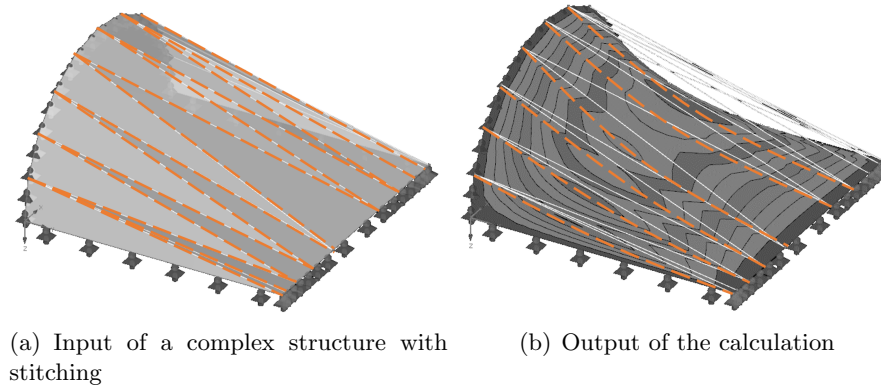


Figure 8-2: Stitching process for modeling a complex structure into *Dlubal RFEM*

software. Following will describe the production, usage and implementation into the static software of these models shown exemplary with the software *Rhino* by *McNeel Europe*.

The outer shape of the structure can be built with simple polylines or curves as is shown in Figure 8-3 (a) on a simple structure. The shape of the membrane is produced by the command *Patch* which will insert a minimal surface with the outer lines as borders which is shown in a simple example in Figure 8-3 (b). However, to ensure that the outer shape is held by the newly produced surface, the option stiffness has to be as small as possible. Is the stiffness chosen to small, the software will produce bad results as well, so there has to be made an approximation.

To transfer the newly produced surface into a static software, the surface has to be exported in the Standard for the Exchange of Product Model Data (STEP) format in the option *AP214AutomotiveDesign*, which can be imported and utilized by the software (see Figure 8-3 (c)).

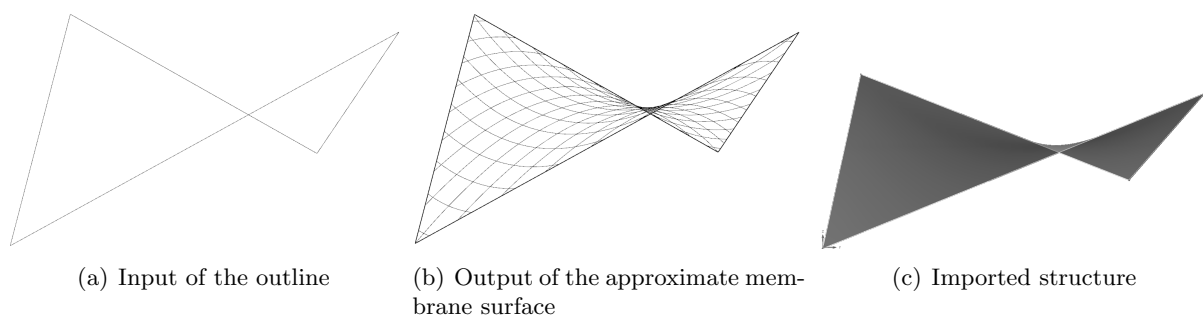


Figure 8-3: Modeling of a simple structure in *Rhino* and its input in a static software

The biggest benefit of the modeling in a special software is, that there is only one surface for the membrane-member, which is not interrupted by stitching lines, that prevent calculations in that area. Therefore, the whole structure and its various values for stresses and deformation can be calculated. An example for a more complex system is shown in Figure 8-4 from the outer shape till the final structure in a finite element software.

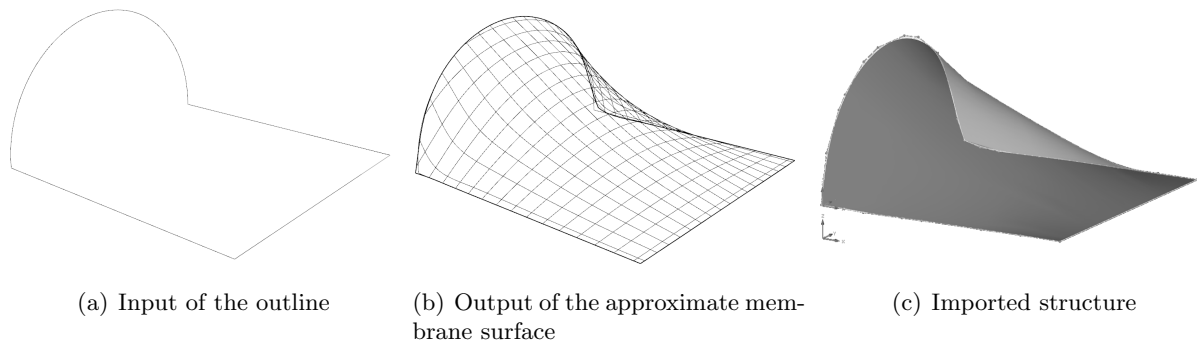


Figure 8-4: Modeling of a complex structure in Rhino and its input in a static software

After the import of the structure, the form-finding Add-in has to be activated in the *basic settings* of the file. Also it is now possible to form any desired bearings and loadings. The pretensioning of the membrane can also be changed initially only isotropic, however after the definition of the axes it can also be inserted as anisotropic stresses. For the correct calculation of the system the type of the form-finding analysis has to be chosen (see Chapter 4.2.2). The whole process is also shown in Figure 8-5:

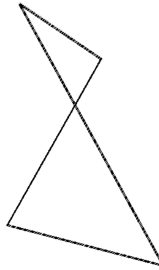
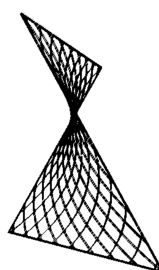

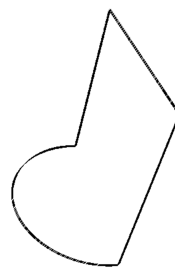
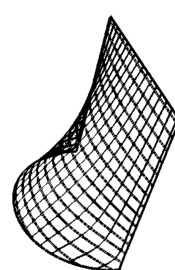
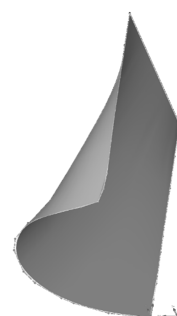
Rhino			RFEM	
Modellieren		Export	Import	Einarbeitung
Äußere Linien der Membranoberfläche zeichnen	Erstellen der Membranoberfläche	<ul style="list-style-type: none"> - Befehl: Export - STEP-Format - Option: AP214-Automotive-Design 	<ul style="list-style-type: none"> - Einheiten: automatisch - Ignoriere freie Linien - Konvertiere NURBS-Flächen zu Quad Flächen - Konvertiere TRIMM-Flächen zu Quad-Flächen 	<ul style="list-style-type: none"> - aktivieren des RF-Formfindung Modules in den Basisangaben - (wenn benötigt: definieren der Hauptachsen in der Datei neu) - definieren der Oberfläche als Membran - definieren der Hauptachsen in der neuen Struktur - definieren der Lagerung des Tragwerkes - Wahl der korrekten Berechnungsmethode <ul style="list-style-type: none"> o Projektionsmethode: hohe konische Tragwerke o Zugmethode: Tragwerke gelagert auf Punkten, Linien, Bögen und pneumatische Strukturen - einbringen der Vorspannung - aufrufen der Belastung - Berechnung (wenn die Software nicht genügend Iterationsschritte durchführt, die Anzahl der Schritte erhöhen)
Einfaches Tragwerk				
				

Figure 8-5: Procedure of the import and export of a generated model

9 Determination of Stresses with an Iterative Calculation

Following will introduce two different approaches to determine stresses for membrane structures.

9.1 Non-Linear Approaches

This non-linear approach takes several different impacts into account and will also consider linear elongation of the membrane due to stresses. It uses the non-linear rope equations which were introduced by Palkowski: [23, p.10]

Load-bearing direction:

$$n_l^3 + n_l^2 \cdot b_l - c_l = 0$$

With:

$$b_l = (EA)_l \cdot \left[1 - \frac{1}{L_{l,s,0}} \cdot (L_l - \alpha_T \cdot \Delta T \cdot L_{l,s,0}) \right]$$

$$c_l = \frac{(EA)_l \cdot (p + q)^2 \cdot L_l^3}{24 \cdot L_{l,s,0}}$$

$$L_{l,0} = L_l \cdot \left(1 + \frac{8 \cdot f_l^2}{3 \cdot L_l^2} \right)$$

Tensioning direction:

$$n_t^3 + n_t^2 \cdot b_t - c_t = 0$$

With:

$$b_t = (EA)_t \cdot \left[1 - \frac{1}{L_{t,s,0}} \cdot (L_t - \alpha_T \cdot \Delta T \cdot L_{t,s,0}) \right]$$

$$c_t = \frac{(EA)_t \cdot (p - q)^2 \cdot L_t^3}{24 \cdot L_{t,s,0}}$$

$$L_{t,s,0} = L_t \cdot \left(1 + \frac{8 \cdot f_t^2}{3 \cdot L_t^2} \right)$$

To solve these problems Palkowski also gives an approximation formula based on the *Newton Approach* which promises a fast convergence using an iteration process:

$$n_1 = q \cdot L \cdot \sqrt{\frac{l}{24 \cdot (s_0 \cdot (1 + \alpha_T \cdot \Delta T) - L)}}$$

Another approximation that can be made is:

$$n_1 \approx n_{membran} \cdot t_{membran}$$

Newton Approach:

$$n_{i+1} = \frac{2 \cdot n_i^3 + b \cdot n_i^2 + c}{3 \cdot n_i^2 + 2 \cdot b \cdot n_i}$$

The iteration process comes to an end, when two successive steps have approximately the same result.

However, this approach was not taken into further account as the following approach gives the more reliable, give more controllable results and is easier to understand due to its clear calculation steps.

9.2 Linear Approach

Whereas the process of determining stresses for membrane structures is highly complex and non-linear, this approach overcomes this with an iteration process, that finds for every step a new equilibrium of the shape depended on the effective stresses, prestress or stresses caused by additional live loads. This approach will be introduced and will be used from now on.

This process uses Theory II. and the so called κ -procedure, that divides the live load into load bearing and tensioning direction according to the geometry of the system. The process of determining stresses is free of any material characteristics except the ratio of stiffness of each main axis.

9.2 Iteration Process: Form-Finding and Calculation of Stresses

The iteration process determines the stresses in the membrane caused by the live load and adds it up to the constant prestress of the membrane for each step anew. When two successive iteration steps have practically the same results the iteration process stops. However, due to unfortunate constellations of numbers it is possible, that the iteration process fails and does not converge. Therefore, it is prudent to examine not only one dead load q but a series of different ones.

Geometry of Equilibrium

The first part of each iteration step is to determine the geometry of equilibrium of the current system, which depends on the ratio of the pretensioning forces in each direction as they influences the curvatures and therefore the sags of load-bearing and tensioning directions. For example a higher force alongside the load-bearing direction will cause the membrane to ascend. This can be derived with following two assumptions:

- the product of stress times the curvature is always equal for both directions

$$n_l \cdot k_l \stackrel{!}{=} n_t \cdot k_t$$

- both sags added together are the total height of the system

$$H = f_l + f_t = \frac{L_l^2}{8 \cdot R_l} + \frac{L_t^2}{8 \cdot R_t}$$

Since the reciprocal of the curvature is the radius, the first assumption can be transformed into:

$$\frac{n_l}{R_l} = \frac{n_t}{R_t}$$

Which gives:

$$R_t = R_l \cdot \frac{n_t}{n_l}$$

Then R_t can be substituted into the second assumption to give following equation:

$$H = \frac{L_l^2}{8 \cdot R_l} + \frac{L_t^2}{8 \cdot R_l \cdot \frac{n_t}{n_l}}$$

Solving this equation for R_l or R_t respectively, leads to Equations 9.1 and 9.2:

$$\frac{1}{k_{l,i}} = R_{l,i} = \frac{L_l^2 \cdot n_{p,t,i} + L_t^2 \cdot n_{p,l,i}}{8 \cdot H \cdot n_{p,t,i}} \quad (9.1)$$

or

$$\frac{1}{k_{t,i}} = R_{t,i} = \frac{L_l^2 \cdot n_{p,l,i} + L_t^2 \cdot n_{p,t,i}}{8 \cdot H \cdot n_{p,t,i}} = R_{t,0,i} \cdot \frac{n_{p,t,i}}{n_{p,l,i}} \quad (9.2)$$

With the mathematical changing of the radii, the sags will change as well. However, according to assumption two, the sum of both sags will always add up to the total height:

$$f_{l,i} = \frac{L_l^2}{8 \cdot R_{l,i}} \quad (9.3)$$

and

$$f_{t,i} = \frac{L_t^2}{8 \cdot R_{t,i}} = H - f_{l,i} \quad (9.4)$$

Though the geometry of equilibrium has to be calculated repeatedly for every step of the iteration process, it is only a mathematical approach and will not give the actual results for the sags. The actual ones are usually close to the geometry of equilibrium without any live load q . The further difference in shape comes from elastic elongation and shortening of the material depending on the direction and loading (cf. Equation 3.1). [4, p.166-167]

κ -Procedure

The κ -procedure determines the division of the force q in load-bearing and tensioning directions depending on the geometry solely to determine factors like G as a geometry factor or κ for the actual force-division.

The geometry factor G depends on the shape and type of loading. Figure 9-1 shows exemplary several different types of possible load cases on a simple rope system and the deformation they will cause, which is called an alysoid, which can be described in different mathematical functions: [24, p. 27-34]

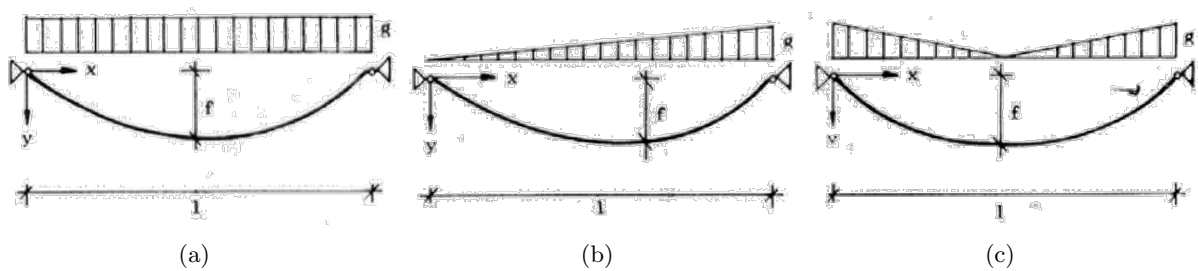


Figure 9-1: Exemplary alysoid for different load cases [24, p.27]

(a) Alysoid under a uniformly distributed load

$$y(x) = \frac{4 \cdot f}{L} \cdot x^2 - \frac{4 \cdot f}{L} \cdot x$$

(b) Alysoïd under a triangular distributed load

$$y(x) = f \cdot \frac{2.6 \cdot x}{L} \cdot \left(1 - \frac{x^2}{L^2}\right)$$

(c) Alysoïd under two triangular distributed load

$$y(x) = f \cdot \frac{2 \cdot x}{L} \cdot \left(3 - 6 \cdot \frac{x}{L} + 4 \cdot \frac{x^2}{L^2}\right)$$

To develop the geometry factor, the actual length of the alysoïd has to be determined by using a formula of line integration:

$$L' = \int_0^L (1 + (y(x)')^2) dx$$

The geometry factor for case (a), the uniformly distributed load will be shown exemplary:

$$y(x)' = \frac{8 \cdot f}{l^2} \cdot x - \frac{4 \cdot f}{l}$$

$$L' = \int_0^L (1 + (y(x)')^2) dx = L \cdot \left(1 + \frac{16 \cdot f^2}{3 \cdot L^2}\right)$$

Hence, the result is factorized with L , the geometry factors G_l and G_t are:

$$G_{l,i} = 1 + \frac{3 \cdot L_l^2}{16 \cdot f_{l,i}^2} \quad (9.5)$$

and

$$G_{t,i} = 1 + \frac{3 \cdot L_t^2}{16 \cdot f_{t,i}^2} \quad (9.6)$$

The force-distribution factor ρ depends on the ratio stiffness of the membrane as well as its geometry-factors G . With the force-distribution factor ρ the actual division of the forces can be calculated with the determination of the κ -factors.

$$\rho_{l,i} = \frac{(EA)_l \cdot G_{t,i} \cdot L_{t,i}^2}{(EA)_t \cdot G_{l,i} \cdot L_{l,i}^2} \quad \Rightarrow \quad \kappa_{l,i} = \frac{1}{1 + \rho_{l,i}} \quad (9.7)$$

and

$$\rho_{t,i} = \frac{(EA)_t \cdot G_{l,i} \cdot L_{l,i}^2}{(EA)_l \cdot G_{t,i} \cdot L_{t,i}^2} \Rightarrow \kappa_{t,i} = \frac{1}{1 + \rho_{t,i}} \quad (9.8)$$

With the usage of the κ -factors, the area loading q can be divided into linear loads along each main-direction by multiplying q with κ for each direction.

$$q_{l,i} = q \cdot \kappa_{l,i} \quad (9.9)$$

and

$$q_{t,i} = q \cdot \kappa_{t,i} \quad (9.10)$$

Stresses caused by Load

The load q or rather $q_{l,i}$ and $q_{t,i}$ respectively are perpendicular to the surface of the membrane. Therefore, the stresses alongside the membrane can be calculated for further calculations. Each of these forces are affiliated with restrictions, which will be discussed later on more precisely.

$$n_{q,l,i} = \frac{q_{l,i} \cdot L_l^2}{8 \cdot f_{l,i}} \quad (9.11)$$

and

$$n_{q,t,i} = \frac{q_{t,i} \cdot L_t^2}{8 \cdot f_{t,i}} \quad (9.12)$$

Remaining Stresses

Until now the pretensioning stresses and the stresses caused by loading were examined separately. In the next step however, they will be assembled to the remaining stresses in the membrane. The load q will cause an increase of stresses along the direction of load-bearing, but at the same time decrease along the tensioning direction.

$$n_{p,l,i+1} = n_{p,l,0} + n_{q,l,i} \quad (9.13)$$

and

$$n_{p,t,i+1} = n_{p,t,0} - n_{q,t,i} \quad (9.14)$$

The last step of each iteration step process is to determine, when the calculations come to a sufficiently exact value. This is the case, when the results of the Equations 9.13 and 9.14 from two successive iteration steps will be approximately equal.

$$n_{p,l,i} \overset{!}{\approx} n_{p,l,i+1} \quad (9.15)$$

and

$$n_{p,t,i} \overset{!}{\approx} n_{p,t,i+1} \quad (9.16)$$

Pretensioning Forces

For further examination, the pretensioning stresses at the beginning are be divided into load-bearing $n_{p,l,0}$ and pretensioning $n_{p,t,0}$ direction. However, these forces can be converted into the vertical forces $p_{l,0}$ and $p_{t,0}$ with Equations 9.17 and 9.18:

$$p_{l,i} = \frac{8 \cdot n_{p,l,i} \cdot f_{l,i}}{L_l^2} \quad (9.17)$$

and

$$p_{t,i} = \frac{8 \cdot n_{p,t,i} \cdot f_{t,i}}{L_t^2} \quad (9.18)$$

Restrictions for Results

The whole iteration process from Equation 9.1 to 9.16 is bound to several restrictions to ensure its accuracy.

- To maintaining the tensile strength of the membrane, the stresses in the load-bearing direction have to be smaller then the tensile strength of the membrane:

$$n_{p,l,i+1} \overset{!}{<} f_{membrane} \quad (9.19)$$

- To ensure the functionality of the system, the stress along the tensioned direction have to be greater then 0 all the time. Sometimes the iteration process will deliver unrealistic results for higher loadings, therefore another examination is needed to eliminate those mistakes. The result of Equation 9.18 has to be greater then the loading $q_{t,i}$ (cf. Figures 4-2 and 4-3):

$$n_{p,t,i+1} \overset{!}{>} 0 \quad (9.20)$$

and

$$p_{t,0} \stackrel{!}{<} q_{t,i} \quad (9.21)$$

- As previously mentioned is it also advisable to calculate the system for a range of loadings q , to visualize and reveal potential mistakes caused by numerical issues, such as division by zero or unlucky constellations of numbers.

9.2 System Requirements

The equations above are restricted to following characteristics of the structure:

- clearly divided in orthogonal load-bearing (l) and tensioning (t) directions
- the ratio of total height to length has to be bigger than 0.25 in all directions, otherwise can the correction of the results not be guaranteed, which was found out by trial and error.

It can be claimed that the higher the ratio, the better the later results.

$$\frac{H}{L_l} \stackrel{!}{>} 0.25 \quad (9.22)$$

$$\frac{H}{L_t} \stackrel{!}{>} 0.25 \quad (9.23)$$

The calculations are free of any material characteristics, only the Young's Modulus and therefore the stiffness in each direction is required, to determine the segregation of forces inside the system:

- Stiffness in load-bearing direction $(EA)_l$
- Stiffness in tensioning direction $(EA)_t$

9.2 Soft Edges

The following part will describe the design process of *soft edges*.

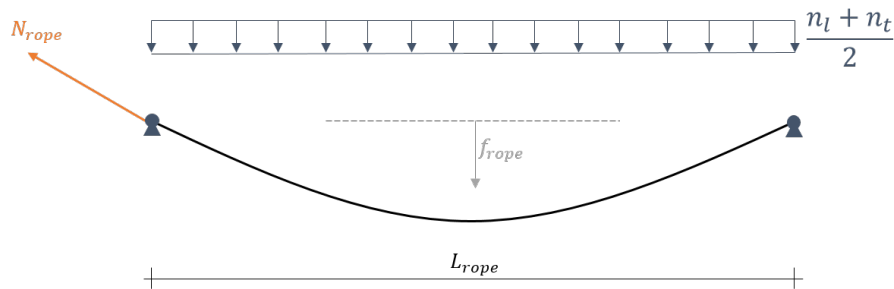


Figure 9-2: Geometry of edge ropes

The first step is to determine the required sag f_{rope} of the edge. Usually it is about one eighth of the span, however this value can be chosen randomly with the factor s_{sag} :

$$f_{rope} = s_{sag} \cdot L_{rope} \quad (9.24)$$

The next step is to determine the required pretensioning force N_{rope} in the rope, to receive the chosen sag. This was derived with an analogy of a simple rope system, where the approximately the average of both pretensioning stresses is taken as the linear loading (cf. Figure 9-2).

The force N_{rope} can be determined by calculating the horizontal and vertical forces H_{rope} and V_{rope} and then using Pythagoras' Theorem as is shown in Figure 9-3.

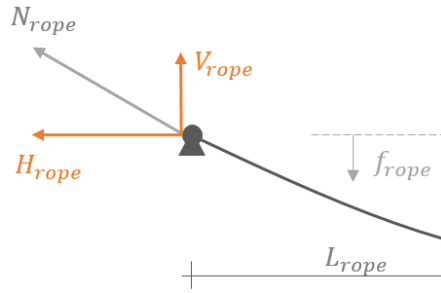


Figure 9-3: Calculation of the force N_{rope}

Therefore, the horizontal forces H can be calculated with

$$H_{rope} = \frac{1}{f_{rope}} \cdot \frac{\frac{n_l + n_t}{2} \cdot L_{rope}^2}{8}$$

and the vertical forces can be determined by using following equation

$$V_{rope} = \frac{\frac{n_l + n_t}{2} \cdot L_{rope}}{2}$$

With Equation 9.25 the absolute value of of those vectors and therefore the force N_{rope} can be calculated, which is also equal to the force at each support of the rope.

$$N_{rope} \approx L_{rope} \cdot \frac{\frac{n_l + n_t}{2}}{f_{rope}} \cdot \sqrt{16 \cdot f_{rope}^2 + L_{rope}} \quad (9.25)$$

9.3 Results

As previously mentioned it is recommended to calculate the stresses with the iteration process for several different loadings to reduce possible mistakes. Therefore, the Figures 9-4 and 9-5 are showing possible results of the iteration process for n_l and n_t for a structure subjected to loadings q from 0 to $2.5 \frac{kN}{m^2}$. The results are also compared to other values determined with an

finite element software.

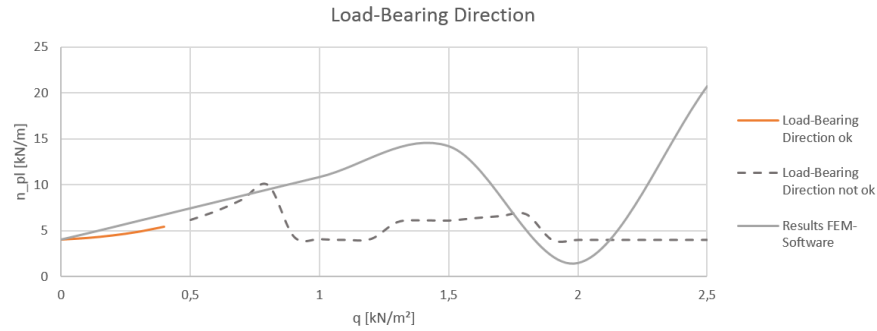


Figure 9-4: Results of n_l of the iteration process for various loadings q

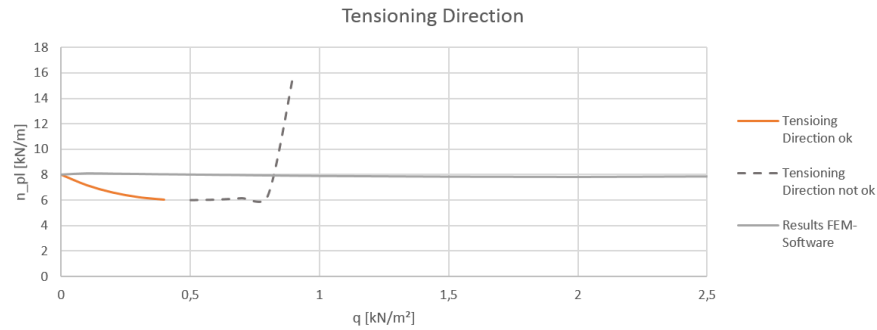


Figure 9-5: Results of n_t of the iteration process for various loadings q

The solid orange line indicates the usable results which were determined by the use of the restrictions from the Equations 9.19, 9.20 and 9.21. The dotted black lines show the remaining non-usable results calculated by the iteration process, which are showing their highly non-linear behavior for higher loadings. The solid gray lines show the results calculated by a finite element software.

It can be seen, that the results calculated in the iteration process and the ones from the finite element software are in the usable section in the acceptance range of approximately 20 to 30% and drift apart irregularly in the non-usable section.

9.4 Exemplary Process

Following will show an exemplary application of the iteration process.

Geometry

- $L_l = 10.00m$
- $L_t = 10.00m$
- $H = 3.00m$

Materials

$$- (EA)_l = (EA)_t$$

Pretensioning Forces

$$- n_{p,l} = 4,00 \frac{kN}{m}$$

$$- n_{p,t} = 8,00 \frac{kN}{m}$$

Loading

The system will be investigated for the loading q . However, it is recommended to investigate it for several different loadings, to point out eventual continuous mistakes of calculation.

$$q = 0,20 \frac{kN}{m^2}$$

9.4 Check of the System

The first step is to determine the requirements of the system to ensure the applicability of the iteration process:

- orthogonal directions? ✓

- ratio of height to length:

$$\frac{H}{L_l} = \frac{3.0m}{10.0m} = 0.3$$

✓

$$\frac{H}{L_t} = \frac{3.0m}{10.0m} = 0.3$$

✓

9.4 Iteration Process

Step 0

Geometry of equilibrium:

$$R_{l,0} = \frac{L_l^2 \cdot n_{p,t,0} + L_t^2 \cdot n_{p,l,0}}{8 \cdot H \cdot n_{p,t,0}} = \frac{10.0^2 \cdot 8.0 + 10.0^2 \cdot 4.0}{8 \cdot 3.0 \cdot 8.0} = 6.25m$$

$$R_{t,0} = R_{l,0} \cdot \frac{n_{p,t,0}}{n_{p,l,0}} = 6.25 \cdot \frac{8.0}{4.0} = 12.5m$$

$$f_{l,0} = \frac{L_l^2}{8 \cdot R_l} = \frac{10.0^2}{8 \cdot 6.25} = 2.0m$$

$$f_{t,0} = H - f_{l,0} = 3.0 - 1.5 = 1.0m$$

κ -Procedure (load distribution):

$$G_{l,0} = 1 + \frac{3 \cdot L_l^2}{16 \cdot f_{l,0}} = 1 + \frac{3 \cdot 10.0^2}{16 \cdot 2.0} = 5.69$$

$$G_{t,0} = 1 + \frac{3 \cdot L_t^2}{16 \cdot f_{t,0}} = 1 + \frac{3 \cdot 10.0^2}{16 \cdot 1.0} = 19.75$$

$$\rho_{l,0} = \frac{(EA)_l \cdot G_{t,0} \cdot L_t^2}{(EA)_t \cdot G_{l,0} \cdot L_l^2} = \frac{(EA)_l \cdot 5.69 \cdot 10.0^2}{(EA)_t \cdot 19.75 \cdot 10.0^2} = 3.47$$

$$\rho_{t,0} = \frac{(EA)_t \cdot G_{l,0} \cdot L_l^2}{(EA)_l \cdot G_{t,0} \cdot L_t^2} = \frac{(EA)_t \cdot 9.33 \cdot 10.0^2}{(EA)_l \cdot 9.33 \cdot 10.0^2} = 0.29$$

$$\kappa_{l,0} = \frac{1}{1 + \rho_{l,0}} = \frac{1}{1 + 3.47} = 0.22$$

$$\kappa_{t,0} = \frac{1}{1 + \rho_{t,0}} = \frac{1}{1 + 0.29} = 0.78$$

$$q_{l,0} = \kappa_{l,0} \cdot q = 0.22 \cdot 0.2 = 0.04 \frac{kN}{m}$$

$$q_{t,0} = \kappa_{t,0} \cdot q = 0.78 \cdot 0.2 = 0.16 \frac{kN}{m}$$

Determination of stresses caused by load:

$$n_{l,q,0} = \frac{q_{l,0} \cdot L_l^2}{8 \cdot f_l} = \frac{0.04 \cdot 10.0^2}{8 \cdot 2.0} = 0.28 \frac{kN}{m}$$

$$n_{t,q,0} = \frac{q_{t,0} \cdot L_t^2}{8 \cdot f_t} = \frac{0.16 \cdot 10.0^2}{8 \cdot 1.0} = 1.94 \frac{kN}{m}$$

Remaining stresses:

$$n_{p,l,0+1} = n_{p,l,1} = 4.0 + 0.28 = 4.28 \frac{kN}{m}$$

$$n_{p,t,0+1} = n_{p,t,1} = 8.0 - 1.95 = 6.06 \frac{kN}{m}$$

Are the results sufficiently exact?

$$n_{p,l,0} = 4.0 \overset{?}{\approx} 4.28 = n_{p,l,1}$$

$$n_{p,t,0} = 8.0 \overset{?}{\approx} 6.06 = n_{p,t,1}$$

Step 1

Geometry of equilibrium:

$$R_{l,1} = \frac{L_l^2 \cdot n_{p,t,1} + L_t^2 \cdot n_{p,l,1}}{8 \cdot H \cdot n_{p,t,1}} = \frac{10.0^2 \cdot 6.06 + 10.0^2 \cdot 4.28}{8 \cdot 3.0 \cdot 6.06} = 6.25m$$

$$R_{t,1} = R_{t,1} \cdot \frac{n_{p,t,1}}{n_{p,l,1}} = 10.52 \cdot \frac{6.06}{4.28} = 12.50m$$

$$f_{l,1} = \frac{L_l^2}{8 \cdot R_{l,1}} = \frac{10,0^2}{8 \cdot 6.25} = 1.76m$$

$$f_{t,1} = H - f_{l,1} = 3.0 - 1.76 = 1.24m$$

κ -Procedure (load distribution):

$$G_{l,1} = 1 + \frac{3 \cdot L_l^2}{16 \cdot f_{l,1}} = 1 + \frac{3 \cdot 10.0^2}{16 \cdot 1.76} = 7.07$$

$$G_{t,1} = 1 + \frac{3 \cdot L_t^2}{16 \cdot f_{t,1}} = 1 + \frac{3 \cdot 10,0^2}{16 \cdot 1.24} = 13.16$$

$$\rho_{l,1} = \frac{(EA)_l \cdot G_{t,1} \cdot L_t^2}{(EA)_t \cdot G_{l,1} \cdot L_l^2} = \frac{(EA)_l \cdot 13.14 \cdot 10.0^2}{(EA)_t \cdot 7.07 \cdot 10.0^2} = 1.86$$

$$\rho_{t,0} = \frac{(EA)_t \cdot G_{l,0} \cdot L_l^2}{(EA)_l \cdot G_{t,0} \cdot L_t^2} = \frac{(EA)_t \cdot 7.07 \cdot 10.0^2}{(EA)_l \cdot 13.14 \cdot 10.0^2} = 0.54$$

$$\kappa_{l,1} = \frac{1}{1 + \rho_{l,1}} = \frac{1}{1 + 1.86} = 0.35$$

$$\kappa_{t,1} = \frac{1}{1 + \rho_{t,1}} = \frac{1}{1 + 0.54} = 0.65$$

$$q_{l,1} = \kappa_{l,1} \cdot q = 0.35 \cdot 0.2 = 0.07 \frac{kN}{m}$$

$$q_{t,1} = \kappa_{t,1} \cdot q = 0.65 \cdot 0.2 = 0.13 \frac{kN}{m}$$

Determination of stresses caused by load:

$$n_{l,q,1} = \frac{q_{l,1} \cdot L_l^2}{8 \cdot f_l} = \frac{0.07 \cdot 10.0^2}{8 \cdot 1.76} = 0.50 \frac{kN}{m}$$

$$n_{t,q,1} = \frac{q_{t,1} \cdot L_t^2}{8 \cdot f_t} = \frac{0.13 \cdot 10.0^2}{8 \cdot 1.24} = 1.31 \frac{kN}{m}$$

Remaining stresses:

$$n_{p,l,1+1} = n_{p,l,2} = 4.0 + 0.50 = 4.50 \frac{kN}{m}$$

$$n_{p,t,1+1} = n_{p,t,2} = 8.0 - 1.31 = 6.69 \frac{kN}{m}$$

Are the results sufficiently exact?

$$n_{p,l,1} = 4.27 \overset{?}{\approx} 4.50 = n_{p,l,2}$$

$$n_{p,t,1} = 6.06 \overset{?}{\approx} 6.69 = n_{p,t,2}$$

Step 2

Geometry of equilibrium:

$$R_{l,2} = 6.67m, R_{t,2} = 10.37m$$

$$f_{l,2} = 1.79m, f_{t,2} = 1.21m$$

κ -Procedure (load distribution):

$$G_{l,2} = 6.83, G_{t,2} = 13.89$$

$$\rho_{l,2} = 2.04, \rho_{t,2} = 0.49$$

$$\kappa_{l,2} = 0.33, \kappa_{t,2} = 0.67$$

$$q_{l,2} = 0.07 \frac{kN}{m}, q_{t,2} = 0.13 \frac{kN}{m}$$

Determination of stresses caused by load:

$$n_{l,q,2} = 0.46 \frac{kN}{m}, n_{t,q,1} = 1.39 \frac{kN}{m}$$

Remaining stresses:

$$n_{p,l,3} = 4.46 \frac{kN}{m}, n_{p,t,3} = 6.61 \frac{kN}{m}$$

Are the results sufficiently exact?

$$n_{p,l,2} = 4.50 \overset{?}{\approx} 4.46 = n_{p,l,3}$$

$$n_{p,t,2} = 6.69 \overset{?}{\approx} 6.61 = n_{p,t,3}$$

Step 3

Geometry of equilibrium:

$$R_{l,3} = 6.98m, R_{t,2} = 10.34m$$

$$f_{l,3} = 1.79m, f_{t,2} = 1.21m$$

κ -Procedure (load distribution):

$$G_{l,3} = 6.84, G_{t,2} = 13.84$$

$$\rho_{l,3} = 2.02, \rho_{t,2} = 0.49$$

$$\kappa_{l,3} = 0.33, \kappa_{t,2} = 0.67$$

$$q_{l,3} = 0.07 \frac{kN}{m}, q_{t,2} = 0.13 \frac{kN}{m}$$

Determination of stresses caused by load:

$$n_{l,q,3} = 0.46 \frac{kN}{m}, n_{t,q,1} = 1.38 \frac{kN}{m}$$

Remaining stresses:

$$n_{p,l,4} = 4.46 \frac{kN}{m}, n_{p,t,4} = 6.62 \frac{kN}{m}$$

Are the results sufficiently exact?

$$n_{p,l,3} = 4.46 \overset{?}{\approx} 4.46 = n_{p,l,4}$$

$$n_{p,t,3} = 6.61 \overset{?}{\approx} 6.62 = n_{p,t,4}$$

Final Results

Therefore, the stresses caused by the loading q are:

$$n_{p,l,final} = 4.46 \frac{kN}{m}, n_{p,t,final} = 6.62 \frac{kN}{m}$$

As was previously mentioned, it is recommended to examine the system for several different loadings q . These results are shown in Figure 9-6, where the solid orange line shows the usable sector of the loading q , whereas the dotted part is the non-usable sector. Both determined by the application of Equations 9.19 and 9.20.

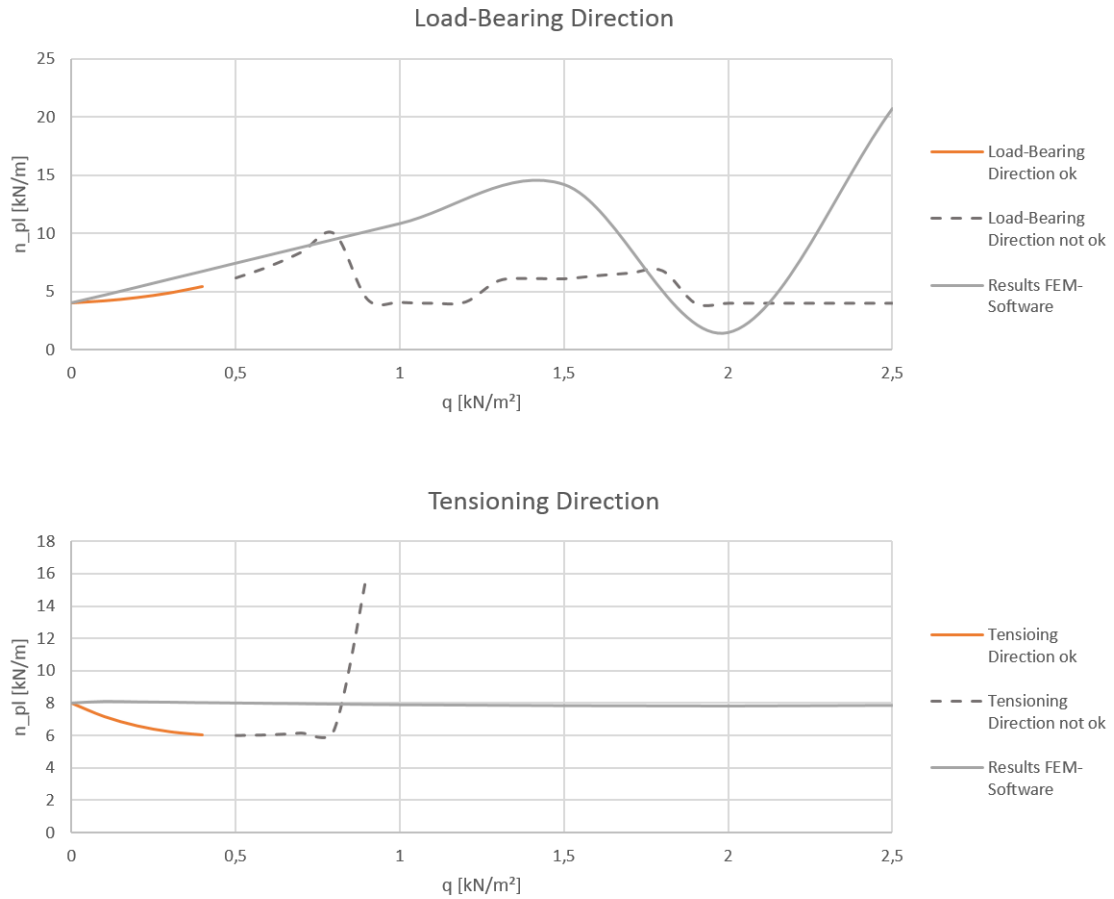


Figure 9-6: Results of $n_{p,l}$ and $n_{p,t}$ for the chosen range of loadings

To get a better idea of the accuracy of the results, close up views of the graphs are shown in Figure 9-7. Both sections show only the usable area of the structure, as for the further loading both approaches give rather accidental results (cf. Figure 9-6). It is also recognizable, that the

results of the iteration process and the ones from the static software are similar in a range of approximately 20% to 30%, when all system requirements are maintained.

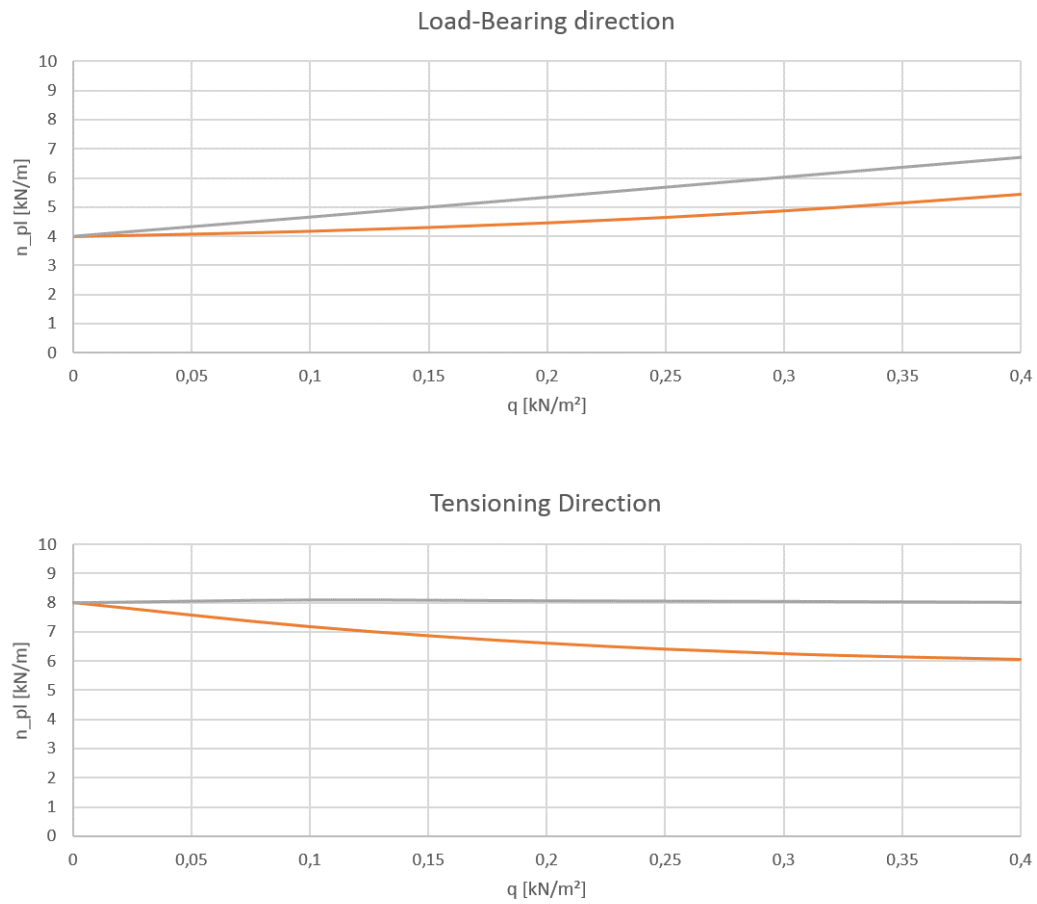


Figure 9-7: Close up view of the results of the iteration process (orange) and the static software *Dlubal RFEM* (grey)

10 Exemplary Calculation

This chapter will show an exemplary design process of a membrane structure. The structure - a roof of a bus station in Pforzheim, Germany (see Figure 10-1) - was designed within the context of a competition by *Planfabrik SPS*. Following will only concentrate on the membranes themselves and not the supporting structure.



Figure 10-1: Visualization of the roofing of the bus station

10.1 System

The structure has a total length of approximately $180.00m$ and a width on one end of $40.30m$ (Figure 10-2) and on the other of $43.90m$ (Figure 10-3) as well as minimum height of $6.90m$ and a maximum height of $9.80m$.

The structure is mounted on a total of 16 slender pillars, which gives the whole light-weight structure a floating-like appearance.

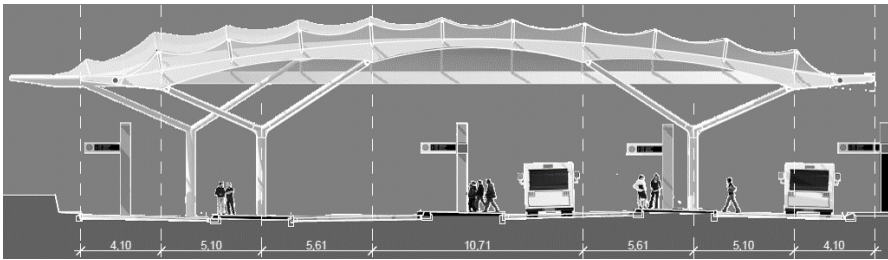


Figure 10-2: Cross section of the roofing on the narrow end

However, the structure can be divided into four differently shaped members, which repeat themselves several times over the building which is also shown in Figure 10-4):

- I **orange:** This member of the structure is mid-field in the broader section and has measurements of approximately: $10.80 \times 3.60 \times 1.10 \text{ m}$
- II **lilac:** This member of the structure is the counterpart of Member I, only in the narrow section of the structure, with approximate measurements of: $11.50 \times 3.60 \times 1.10 \text{ m}$

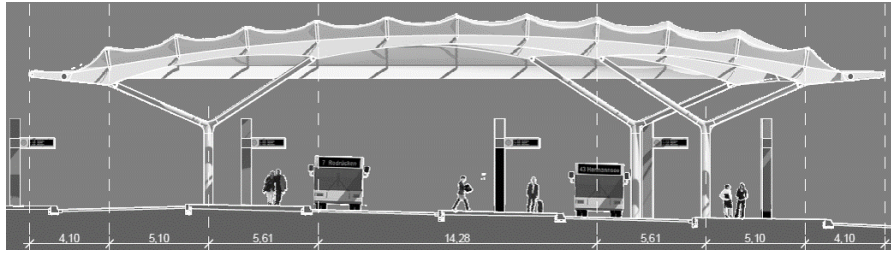


Figure 10-3: Cross section of the roofing on the broad end

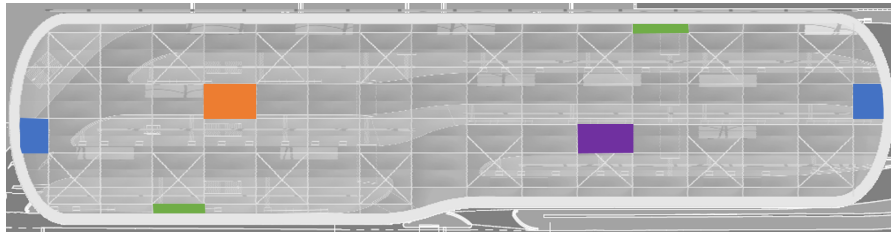


Figure 10-4: Overview of the further investigated parts of the structure

III **blue:** Both ends of the structure are rounded off with the biggest members roughly the same measurements: $6.00 \times 3.55 \times 1.90 \text{ m}$

IV **green:** Lengthways of the structure, it is lined with the same member all along: $1.90 \times 3.60 \times 1.10 \text{ m}$

Modeling

The members I to IV were modeled by using the software Rhino:

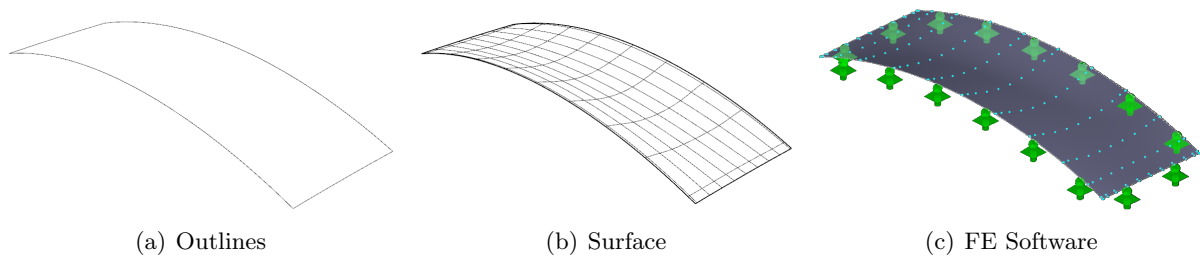


Figure 10-5: Modeling of Member I

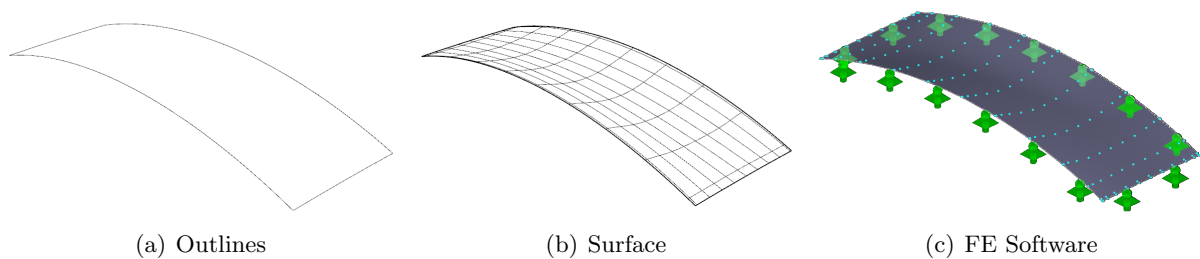


Figure 10-6: Modeling of Member II

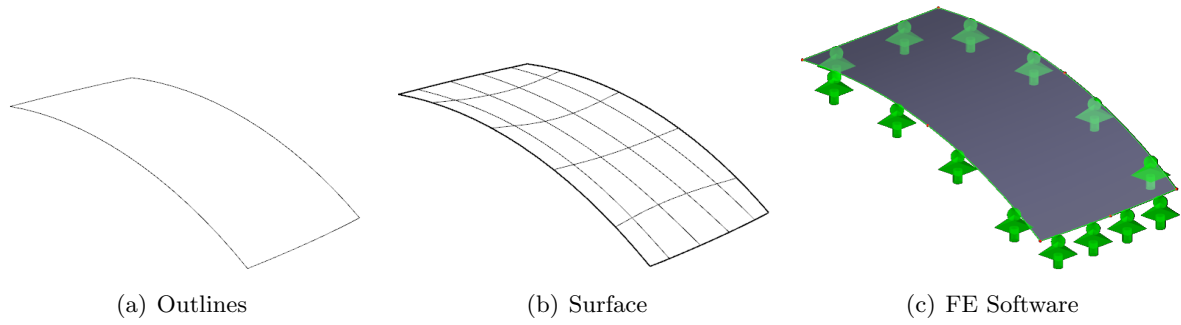


Figure 10-7: Modeling of Member III

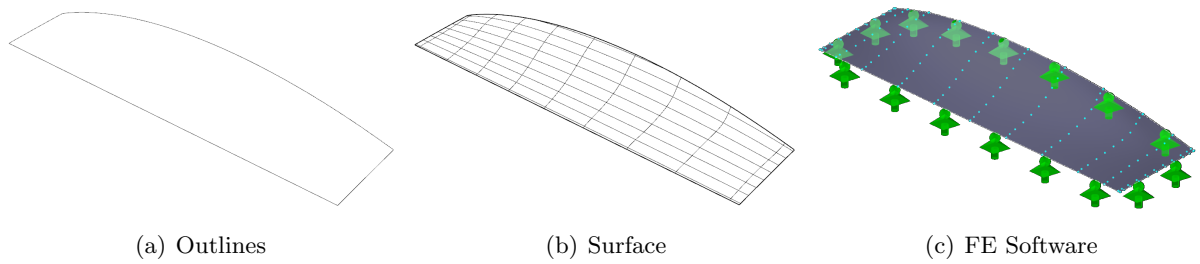


Figure 10-8: Modeling of Member IV

10.2 Loadings

For the preliminary design of the structure following loadings will be approximately determined:

- Snow s
- Down-wind w_{\downarrow}
- Up-wind w_{\uparrow}

Snow s

The determination of the snow-loading was made by the lead of *DIN EN 1991-1-3:2010* including *DIN EN 1991-1-3/NA:2010-12* and the assumption of a double pitch roof.

Characteristics of the location Pforzheim:

- Snowzone 1
- Height: 261m above sea level < 400m → minimum value

$$s_k = 0.65 \frac{kN}{m^2}$$

Characteristics of the structure:

- maximum slope $\approx < 30^\circ \rightarrow \gamma_1 = 0.8$

$$s_c = 0.8 \cdot 0.65 = 0.52 \frac{kN}{m^2}$$

Wind w

The determination of the snow-loading was made by the lead of *DIN EN 1991-1-4:2005* including *DIN EN 1991-1-4/NA:2008-09* and the assumption of a freestanding pitch roof (see Figure 10-9).

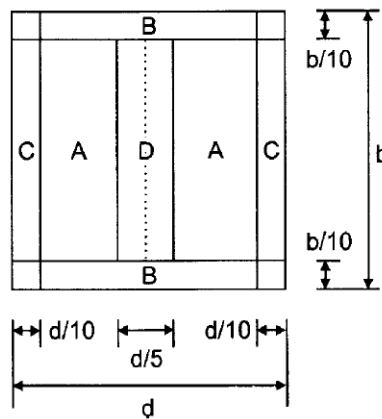


Figure 10-9: Breakdown of the roof area [25, p.326]

Characteristics of the location Pforzheim:

- Windzone 1
- Maximum height structure = 9.80m

$$\rightarrow q_p = 0.50 \frac{kN}{m^2}$$

The loading for up and down wind are determined in Table 10-1, for each section of the structure, in comparison to its weight distributed over the total surface. The values for c_{pe} were determined by Table 7.7 in the code. [20]

Table 10-1: Determination of the wind loading

	Area [m ²]	Angle	$c_{pe,\uparrow}$	$c_{pe,\downarrow}$	$w_{c,\uparrow}$	$w_{c,\downarrow}$
A	1821.6	+10°	-0.7	0.7	-0.08	0.08
		-10°	-0.8	0.6	-0.10	0.07
B	757.8	0°	-1.35	1.65	-0.07	0.08
			-1.35	1.65	-0.07	0.08
C	604.8	+30°	-1.4	1.6	-0.06	0.06
		-30°	-1.6	0.6	-0.06	0.02
D	606.2	+5°	-1.1	0.4	-0.04	0.02
		-5°	-0.6	0.8	-0.02	0.03

To finally calculate the loadings, each section loading has to be added together to get considerable preliminary loadings.

$$w_{c,\uparrow} = -0.50 \frac{kN}{m^2}$$

$$w_{c,\downarrow} = 0.46 \frac{kN}{m^2}$$

Final Loadings

As the death load and therefore the stress n_{DL} is usually very small for membrane structures, it is going to be neglected from now on.

The loading $q_{c,\downarrow}$ has to be determined by following Equation, which considers a combination factor Ψ and probability of a simultaneously acting of wind and snow loadings:

$$q_{c,\downarrow} = \max \begin{cases} s_c + w_{c,\downarrow} \cdot \Psi = 0.52 + 0.46 \cdot 0.2 = 0.612 \frac{kN}{m^2} \\ s_c \cdot \Psi + w_{c,\downarrow} = 0.52 \cdot 0.2 + 0.46 = 0.564 \frac{kN}{m^2} \end{cases}$$

$$q_{c,\downarrow} = 0.612 \frac{kN}{m^2}$$

As the upward wind loading has no other impacts with the same direction of action, there is no combination required.

$$q_{c,\uparrow} = -0.50 \frac{kN}{m^2}$$

10.3 Determining Stresses

Following will show the determination of the pretensioning of the structures as well as the stresses given by the using of the iteration process introduced in Chapter 9.2.1 for the structure-members I to IV.

10.3 Member I

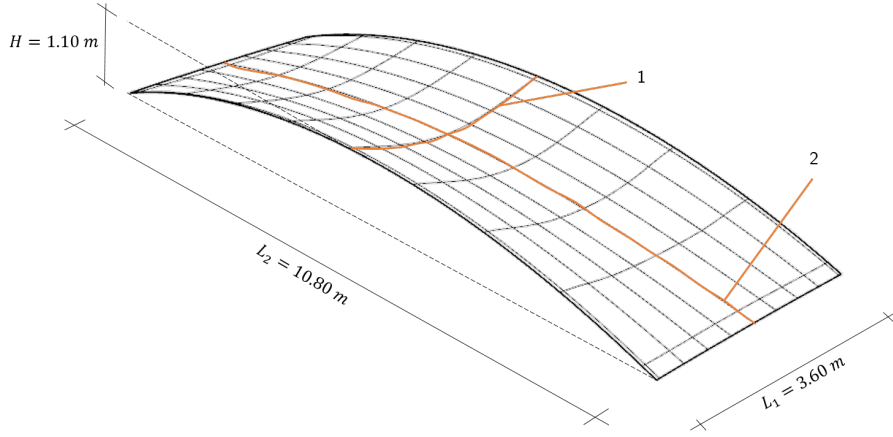


Figure 10-10: Measurements of Member I

Geometries

- Downward forces ↓

$$L_l = 3.60m$$

$$L_t = 10.80m$$

- Upward forces ↑

$$L_l = 10.80m$$

$$L_t = 3.60m$$

Choosing the Pretensioning

To make a preliminary design of the required pretensioning stresses in the membrane Equations 9.11 and 9.12 were used with the usage of the previously determined loadings $q_{c,\downarrow}$ and $q_{c,\uparrow}$ as well as the assumption, that each sag is $\frac{H}{2}$

$$n_{1,member1} \approx \frac{L_l^2 \cdot q_{c,\downarrow}}{8 \cdot f_l} = \frac{10.80^2 \cdot 0.612}{8 \cdot 0.55} = 1.80 \frac{kN}{m}$$

$$n_{2,member1} \approx \frac{L_l^2 \cdot q_{c,\uparrow}}{8 \cdot f_l} = \frac{3.60^2 \cdot 0.50}{8 \cdot 0.55} = 13.25 \frac{kN}{m}$$

To reduce the high ratio between both pretensioning stresses to 0.5, n_2 will be raised, therefore:

$$n_{1,0,member1} = 7.00 \frac{kN}{m}$$

$$n_{2,0,member1} = 14.00 \frac{kN}{m}$$

Stresses for Downward Loading $q_{c,\downarrow}$

For the snow-load $q_{c,\downarrow} = 0.612 \frac{kN}{m^2}$ the iteration process gives following stresses (including pre-tensioning):

- $n_{l,c} = n_{1,iteration} = 14.46 \frac{kN}{m}$
- $n_{t,c} = n_{2,iteration} = 10.78 \frac{kN}{m}$

Which leads to following stresses caused by the loading:

- $n_{l,q,c} = n_{l,p,c} - n_{1,0,member1} = 14.46 - 7.00 = 7.46 \frac{kN}{m}$
- $n_{t,q,c} = n_{t,p,c} - n_{2,0,member1} = 10.78 - 14.00 = -3.22 \frac{kN}{m}$

Proofing Stresses for $q_{c,\downarrow}$

- Short-time strength for $20^\circ C$

$$\begin{aligned} n_{0,Ed} &= 1.35 \cdot n_{DL} + 1.00 \cdot n_p + 1.50 \cdot n_q \\ &= 0 + 1.0 \cdot 7.00 + 1.50 \cdot 7.46 = 18.19 \frac{kN}{m} \stackrel{!}{<} perm.n_{0,Rd} \end{aligned}$$

- Short-time strength for $70^\circ C$

$$\begin{aligned} n_{\vartheta,Ed} &= 1.00 \cdot n_{DL} + 1.00 \cdot n_p + 1.50 \cdot n_q \\ &= 0 + 1.0 \cdot 7.00 + 1.50 \cdot 7.46 = 18.19 \frac{kN}{m} \stackrel{!}{<} perm.n_{\vartheta,Rd} \end{aligned}$$

- Long-time strength for $20^\circ C$

$$\begin{aligned} n_{t,Ed} &= 1.35 \cdot n_{DL} + 1.50 \cdot n_p \\ &= 0 + 1.50 \cdot 7.00 = 10.50 \frac{kN}{m} \stackrel{!}{<} perm.n_{t,Rd} \end{aligned}$$

Stresses for Upwards Loading $q_{c,\uparrow}$

For the wind-load $q_{c,\uparrow} = -0.50 \frac{kN}{m^2}$ the iteration process gives following stresses (including pre-tensioning):

- $n_{s,p,c} = 22.28 \frac{kN}{m}$
- $n_{s,p,c} = 6.77 \frac{kN}{m}$

Which leads to following stresses caused by the loading:

- $n_{s,p,c} = 22.28 - 14.00 = 8.28 \frac{kN}{m}$
- $n_{s,p,c} = 6.77 - 7.00 = -0.23 \frac{kN}{m}$

Proofing Stresses for $q_{c,\uparrow}$

- Short-time strength for $20^\circ C$

$$n_{0,Ed} = 1.35 \cdot n_{DL} + 1.00 \cdot n_p + 1.50 \cdot n_q$$

$$= 0 + 1.0 \cdot 14.00 + 1.50 \cdot 8.28 = 26.42 \frac{kN}{m} \stackrel{!}{<} perm.n_{0,Rd}$$
- Short-time strength for $70^\circ C$

$$n_{\vartheta,Ed} = 1.00 \cdot n_{DL} + 1.00 \cdot n_p + 1.50 \cdot n_q$$

$$= 0 + 1.00 \cdot 14.00 + 1.50 \cdot 8.28 = 26.42 \frac{kN}{m} \stackrel{!}{<} perm.n_{\vartheta,Rd}$$
- Long-time strength for $20^\circ C$

$$n_{t,Ed} = 1.35 \cdot n_{DL} + 1.50 \cdot n_p$$

$$= 0 + 1.00 \cdot 14.00 = 21.00 \frac{kN}{m} \stackrel{!}{<} perm.n_{t,Rd}$$

Comparison with RFEM

Determining the stresses for Member I with the Finite Element Software *RFEM* gives following values:

- Stresses for $q_{c,\downarrow}$

$$n_{l,RFEM} = 15.04 \frac{kN}{m} \quad \rightarrow \text{Difference: } 1 - \frac{14.46}{15.04} = 3.9\%$$

$$n_{t,RFEM} = 3.62 \frac{kN}{m} \quad \rightarrow \text{Difference: } 1 - \frac{10.78}{3.62} = -177.8\%$$
- Stresses for $q_{c,\uparrow}$

$$n_{l,RFEM} = 14.24 \frac{kN}{m} \quad \rightarrow \text{Difference: } 1 - \frac{22.28}{14.24} = -56.5\%$$

$$n_{t,RFEM} = 10.39 \frac{kN}{m} \quad \rightarrow \text{Difference: } 1 - \frac{10.78}{10.39} = -3.8\%$$

10.3 Member II

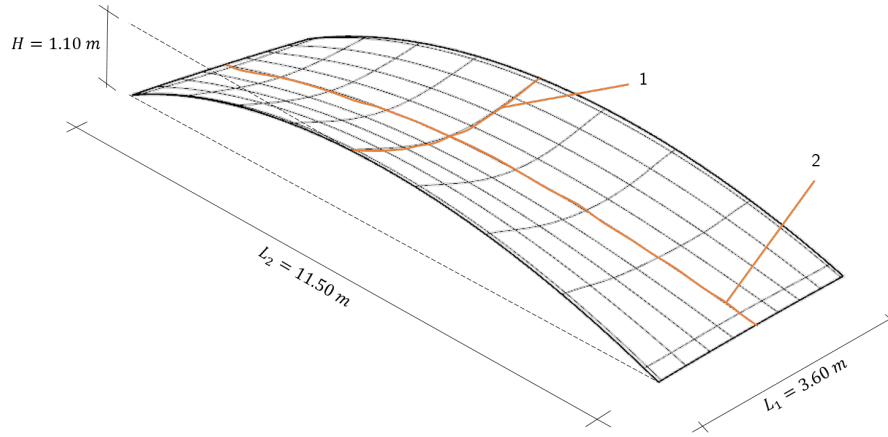


Figure 10-11: Measurements of Member II

Geometries

- Downward forces ↓

$$L_l = 3.60m$$

$$L_t = 11.50m$$

- Upward forces ↑

$$L_l = 11.50m$$

$$L_t = 3.60m$$

Choosing the Pretensioning

To make a preliminary design of the required pretensioning stresses in the membrane Equations 9.11 and 9.12 were used with the usage of the previously determined loadings $q_{c,\downarrow}$ and $q_{c,\uparrow}$ as well as the assumption, that each sag is $\frac{H}{2}$

$$n_{1,member2} \approx \frac{L_l^2 \cdot q_{c,\downarrow}}{8 \cdot f_l} = \frac{11.50^2 \cdot 0.612}{8 \cdot 0.55} = 1.8 \frac{kN}{m}$$

$$n_{2,member2} \approx \frac{L_l^2 \cdot q_{c,\uparrow}}{8 \cdot f_l} = \frac{3.60^2 \cdot 0.50}{8 \cdot 0.55} = 15.00 \frac{kN}{m}$$

To reduce the high ratio between both pretensioning stresses to 0.5, n_2 will be raised, therefore:

$$n_{1,0,member2} = 8.00 \frac{kN}{m}$$

$$n_{2,0,member2} = 16.00 \frac{kN}{m}$$

Stresses for Downward Loading $q_{c,\downarrow}$

For the snow-load $q_{c,\downarrow} = 0.612 \frac{kN}{m^2}$ the iteration process gives following stresses (including pre-tensioning):

- $n_{l,c} = n_{1,iteration} = 16.05 \frac{kN}{m}$
- $n_{t,c} = n_{2,iteration} = 12.26 \frac{kN}{m}$

Which leads to following stresses caused by the loading:

- $n_{l,q,c} = n_{l,p,c} - n_{1,0,member1} = 16.05 - 8.00 = 8.05 \frac{kN}{m}$
- $n_{t,q,c} = n_{t,p,c} - n_{2,0,member1} = 12.26 - 16.00 = -3.74 \frac{kN}{m}$

Proofing Stresses for $q_{c,\downarrow}$

- Short-time strength for $20^\circ C$

$$\begin{aligned} n_{0,Ed} &= 1.35 \cdot n_{DL} + 1.00 \cdot n_p + 1.50 \cdot n_q \\ &= 0 + 1.0 \cdot 8.00 + 1.50 \cdot 8.05 = 20.08 \frac{kN}{m} \stackrel{!}{<} perm.n_{0,Rd} \end{aligned}$$

- Short-time strength for $70^\circ C$

$$\begin{aligned} n_{\vartheta,Ed} &= 1.00 \cdot n_{DL} + 1.00 \cdot n_p + 1.50 \cdot n_q \\ &= 0 + 1.00 \cdot 8.00 + 1.50 \cdot 8.05 = 20.08 \frac{kN}{m} \stackrel{!}{<} perm.n_{\vartheta,Rd} \end{aligned}$$

- Long-time strength for $20^\circ C$

$$\begin{aligned} n_{t,Ed} &= 1.35 \cdot n_{DL} + 1.50 \cdot n_p \\ &= 0 + 1.50 \cdot 8.00 = 12 \frac{kN}{m} \stackrel{!}{<} perm.n_{t,Rd} \end{aligned}$$

Stresses for Upwards Loading $q_{c,\uparrow}$

For the wind-load $q_{c,\uparrow} = -0.50 \frac{kN}{m^2}$ the iteration process gives following stresses (including pre-tensioning):

- $n_{s,p,c} = 25.04 \frac{kN}{m}$
- $n_{s,p,c} = 7.73 \frac{kN}{m}$

Which leads to following stresses caused by the loading:

- $n_{s,p,c} = 25.04 - 16.00 = 9.04 \frac{kN}{m}$
- $n_{s,p,c} = 7.73 - 8.00 = -0.27 \frac{kN}{m}$

Proofing Stresses for $q_{c,\uparrow}$

- Short-time strength for $20^\circ C$

$$\begin{aligned} n_{0,Ed} &= 1.35 \cdot n_{DL} + 1.00 \cdot n_p + 1.50 \cdot n_q \\ &= 0 + 1.00 \cdot 16.00 + 1.50 \cdot 9.04 = 29.56 \frac{kN}{m} \stackrel{!}{<} perm.n_{0,Rd} \end{aligned}$$

- Short-time strength for $70^\circ C$

$$\begin{aligned} n_{\vartheta,Ed} &= 1.00 \cdot n_{DL} + 1.00 \cdot n_p + 1.50 \cdot n_q \\ &= 0 + 1.00 \cdot 16.00 + 1.50 \cdot 9.04 = 29.56 \frac{kN}{m} \stackrel{!}{<} perm.n_{\vartheta,Rd} \end{aligned}$$

- Long-time strength for $20^\circ C$

$$\begin{aligned} n_{t,Ed} &= 1.35 \cdot n_{DL} + 1.50 \cdot n_p \\ &= 0 + 1.50 \cdot 16.00 = 24 \frac{kN}{m} \stackrel{!}{<} perm.n_{t,Rd} \end{aligned}$$

Comparison with RFEM

Determining the stresses for Member II with the Finite Element Software *RFEM* gives following values:

- Stresses for $q_{c,\downarrow}$

$$n_{l,RFEM} = 16.87 \frac{kN}{m} \quad \rightarrow \text{Difference: } 1 - \frac{16.05}{16.87} = 4.9\%$$

$$n_{t,RFEM} = 4.89 \frac{kN}{m} \quad \rightarrow \text{Difference: } 1 - \frac{12.26}{4.89} = -150.7\%$$

- Stresses for $q_{c,\uparrow}$

$$n_{l,RFEM} = 11.07 \frac{kN}{m} \quad \rightarrow \text{Difference: } 1 - \frac{25.04}{11.07} = -126.2\%$$

$$n_{t,RFEM} = 16.20 \frac{kN}{m} \quad \rightarrow \text{Difference: } 1 - \frac{7.73}{16.20} = 52.3\%$$

10.3 Member III

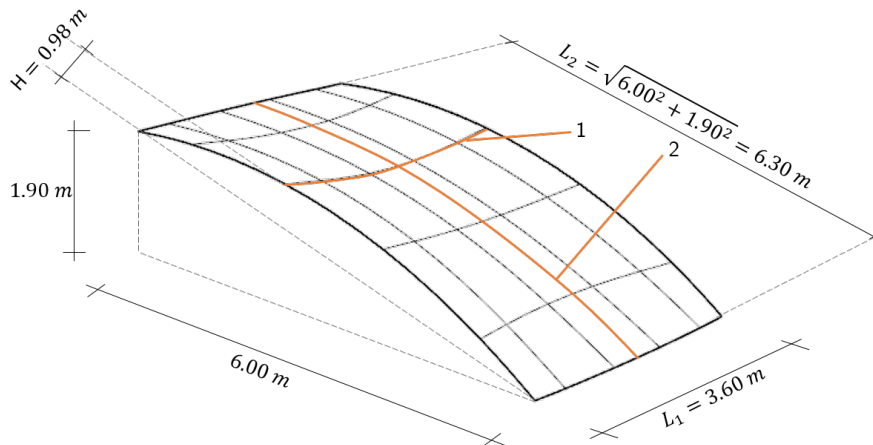


Figure 10-12: Measurements of Member III

Geometries

- Downward forces ↓

$$L_l = 3.60m$$

$$L_t = 6.30m$$

- Upward forces ↑

$$L_l = 6.30m$$

$$L_t = 3.60m$$

Choosing the Pretensioning

To make a preliminary design of the required pretensioning stresses in the membrane Equations 9.11 and 9.12 were used with the usage of the previously determined loadings $q_{c,\downarrow}$ and $q_{c,\uparrow}$ as well as the assumption, that each sag is $\frac{H}{2}$

$$n_{1,member3} \approx \frac{L_l^2 \cdot q_{c,\downarrow}}{8 \cdot f_l} = \frac{3.60^2 \cdot 0.612}{8 \cdot 0.49} = 2.02 \frac{kN}{m}$$

$$n_{2,member3} \approx \frac{L_t^2 \cdot q_{c,\uparrow}}{8 \cdot f_l} = \frac{6.30^2 \cdot 0.50}{8 \cdot 0.49} = 5.06 \frac{kN}{m}$$

To reduce the high ratio between both pretensioning stresses to 0.5, n_2 will be raised, therefore:

$$n_{1,0,member3} = 3.00 \frac{kN}{m}$$

$$n_{2,0,member3} = 6.00 \frac{kN}{m}$$

Stresses for Downward Loading $q_{c,\downarrow}$

For the loading $q_{c,\downarrow} = 0.612 \frac{kN}{m^2}$ the iteration process gives following stresses (including pretensioning):

- $n_{l,c} = n_{1,iteration} = 6.40 \frac{kN}{m}$

- $n_{t,c} = n_{2,iteration} = 4.63 \frac{kN}{m}$

Which leads to following stresses caused by the loading:

- $n_{l,q,c} = n_{l,p,c} - n_{1,0,member1} = 6.40 - 3.00 = 3.40 \frac{kN}{m}$

- $n_{t,q,c} = n_{t,p,c} - n_{2,0,member1} = 4.63 - 6.00 = -1.37 \frac{kN}{m}$

Proofing Stresses for $q_{c,\downarrow}$

- Short-time strength for $20^\circ C$

$$\begin{aligned} n_{0,Ed} &= 1.35 \cdot n_{DL} + 1.00 \cdot n_p + 1.50 \cdot n_q \\ &= 0 + 1.0 \cdot 3.00 + 1.50 \cdot 3.74 = 8.73 \frac{kN}{m} \stackrel{!}{<} perm.n_{0,Rd} \end{aligned}$$

- Short-time strength for $70^\circ C$

$$\begin{aligned} n_{\vartheta,Ed} &= 1.00 \cdot n_{DL} + 1.00 \cdot n_p + 1.50 \cdot n_q \\ &= 0 + 1.0 \cdot 3.00 + 1.50 \cdot 3.74 = 8.73 \frac{kN}{m} \stackrel{!}{<} perm.n_{\vartheta,Rd} \end{aligned}$$

- Long-time strength for $20^\circ C$

$$\begin{aligned} n_{t,Ed} &= 1.35 \cdot n_{DL} + 1.50 \cdot n_p \\ &= 0 + 1.50 \cdot 3.00 = 4.50 \frac{kN}{m} \stackrel{!}{<} perm.n_{t,Rd} \end{aligned}$$

Stresses for Upwards Loading $q_{c,\uparrow}$

For the wind-load $q_{c,\uparrow} = -0.50 \frac{kN}{m^2}$ the iteration process gives following stresses (including pre-tensioning):

- $n_{s,p,c} = 11.39 \frac{kN}{m}$
- $n_{s,p,c} = 2.90 \frac{kN}{m}$

Which leads to following stresses caused by the loading:

- $n_{s,p,c} = 11.39 - 6.00 = 5.39 \frac{kN}{m}$
- $n_{s,p,c} = 2.90 - 3.00 = -0.10 \frac{kN}{m}$

Proofing Stresses for $q_{c,\uparrow}$

- Short-time strength for $20^\circ C$

$$\begin{aligned} n_{0,Ed} &= 1.35 \cdot n_{DL} + 1.00 \cdot n_p + 1.50 \cdot n_q \\ &= 0 + 1.0 \cdot 6.00 + 1.50 \cdot 5.39 = 14.09 \frac{kN}{m} \stackrel{!}{<} perm.n_{0,Rd} \end{aligned}$$

- Short-time strength for $70^\circ C$

$$\begin{aligned} n_{\vartheta,Ed} &= 1.00 \cdot n_{DL} + 1.00 \cdot n_p + 1.50 \cdot n_q \\ &= 0 + 1.00 \cdot 6.00 + 1.50 \cdot 5.39 = 14.09 \frac{kN}{m} \stackrel{!}{<} perm.n_{\vartheta,Rd} \end{aligned}$$

- Long-time strength for $20^\circ C$

$$\begin{aligned} n_{t,Ed} &= 1.35 \cdot n_{DL} + 1.5 \cdot n_p \\ &= 0 + 1.50 \cdot 6.00 = 9.00 \frac{kN}{m} \stackrel{!}{<} perm.n_{t,Rd} \end{aligned}$$

Comparison with RFEM

Determining the stresses for Member III with the Finite Element Software *RFEM* gives following values:

- Stresses for $q_{c,\downarrow}$

$$n_{l,RFEM} = 6.55 \frac{kN}{m} \quad \rightarrow \text{Difference: } 1 - \frac{6.40}{6.55} = 2.3\%$$

$$n_{t,RFEM} = 0.04 \frac{kN}{m} \quad \rightarrow \text{Difference: } 1 - \frac{4.63}{0.04} = -\%$$

- Stresses for $q_{c,\uparrow}$

$$n_{l,RFEM} = 5.78 \frac{kN}{m} \quad \rightarrow \text{Difference: } 1 - \frac{11.39}{5.78} = -97.1\%$$

$$n_{t,RFEM} = 5.78 \frac{kN}{m} \quad \rightarrow \text{Difference: } 1 - \frac{2.90}{5.78} = 49.8\%$$

10.3 Member IV

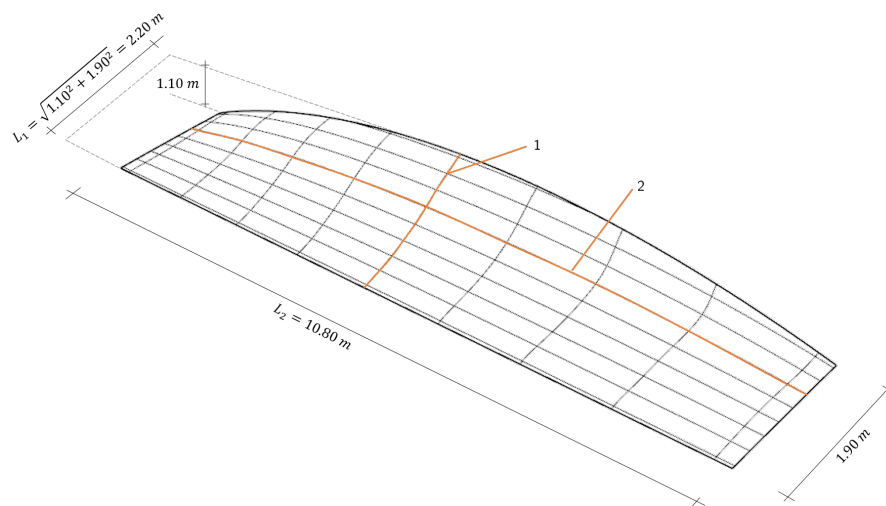


Figure 10-13: Measurements of Member IV

Geometries

- Downward forces \downarrow

$$L_l = 2.20m$$

$$L_t = 10.80m$$

- Upward forces \uparrow

$$L_l = 10.80m$$

$$L_t = 2.20m$$

The actual system height in the middle cross-section of Member IV (see Figure 10-14) is calculated by:

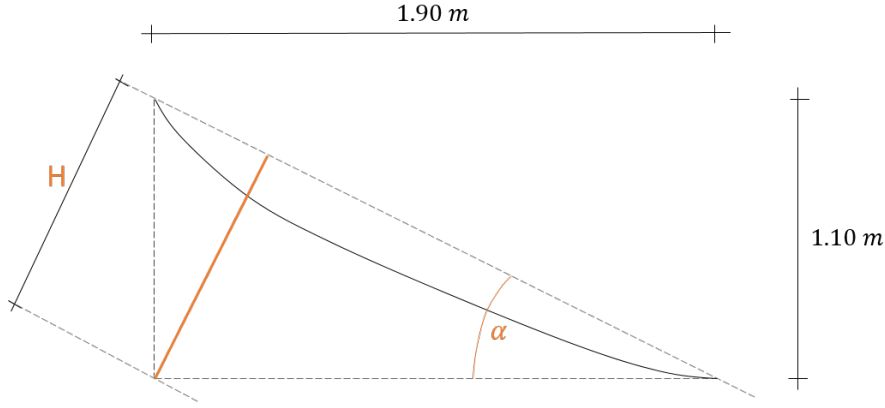


Figure 10-14: Actual Height of Member IV

$$H = \sin(\tan^{-1}(\frac{1.10}{1.90})) \cdot 1.90 = 0.95m$$

Choosing the Pretensioning

To make a preliminary design of the required pretensioning stresses in the membrane Equations 9.11 and 9.12 were used with the usage of the previously determined loadings $q_{c,\downarrow}$ and $q_{c,\uparrow}$ as well as the assumption, that each sag is $\frac{H}{2}$

$$n_{1,member4} \approx \frac{L_l^2 \cdot q_{c,\downarrow}}{8 \cdot f_l} = \frac{2.20^2 \cdot 0.612}{8 \cdot 0.475} = 0.78 \frac{kN}{m}$$

$$n_{2,member4} \approx \frac{L_l^2 \cdot q_{c,\uparrow}}{8 \cdot f_l} = \frac{10.80^2 \cdot 0.50}{8 \cdot 0.475} = 18.90 \frac{kN}{m}$$

To reduce the high ratio between both pretensioning stresses to 0.5, n_2 will be raised, therefore:

$$n_{1,0,member4} = 10.00 \frac{kN}{m}$$

$$n_{2,0,member4} = 20.00 \frac{kN}{m}$$

Stresses for Downward Loading $q_{c,\downarrow}$

For the snow-load $q_{c,\downarrow} = 0.612 \frac{kN}{m^2}$ the iteration process gives following stresses (including pretensioning):

- $n_{l,c} = n_{1,iteration} = 14.61 \frac{kN}{m}$
- $n_{t,c} = n_{2,iteration} = 14.92 \frac{kN}{m}$

Which leads to following stresses caused by the loading:

$$\begin{aligned}
 - n_{l,q,c} &= n_{l,p,c} - n_{1,0,member1} = 14.61 - 10.00 = 4.61 \frac{kN}{m} \\
 - n_{t,q,c} &= n_{t,p,c} - n_{2,0,member1} = 14.92 - 20.00 = -5.08 \frac{kN}{m}
 \end{aligned}$$

Proofing Stresses for $q_{c,\downarrow}$

- Short-time strength for $20^\circ C$

$$\begin{aligned}
 n_{0,Ed} &= 1.35 \cdot n_{DL} + 1.00 \cdot n_p + 1.50 \cdot n_q \\
 &= 0 + 1.00 \cdot 10.00 + 1.50 \cdot 4.61 = 16.92 \frac{kN}{m} \stackrel{!}{<} perm.n_{0,Rd}
 \end{aligned}$$

- Short-time strength for $70^\circ C$

$$\begin{aligned}
 n_{\vartheta,Ed} &= 1.00 \cdot n_{DL} + 1.00 \cdot n_p + 1.50 \cdot n_q \\
 &= 0 + 1.00 \cdot 10 + 1.50 \cdot 4.61 = 16.92 \frac{kN}{m} \stackrel{!}{<} perm.n_{\vartheta,Rd}
 \end{aligned}$$

- Long-time strength for $20^\circ C$

$$\begin{aligned}
 n_{t,Ed} &= 1.35 \cdot n_{DL} + 1.50 \cdot n_p \\
 &= 0 + 1.50 \cdot 10.00 = 15.00 \frac{kN}{m} \stackrel{!}{<} perm.n_{t,Rd}
 \end{aligned}$$

Stresses for Upwards Loading $q_{c,\uparrow}$

For the wind-load $q_{c,\uparrow} = -0.50 \frac{kN}{m^2}$ the iteration process gives following stresses (including pre-tensioning):

$$\begin{aligned}
 - n_{s,p,c} &= 27.67 \frac{kN}{m} \\
 - n_{s,p,c} &= 9.68 \frac{kN}{m}
 \end{aligned}$$

Which leads to following stresses caused by the loading:

$$\begin{aligned}
 - n_{s,p,c} &= 27.67 - 20.00 = 7.68 \frac{kN}{m} \\
 - n_{s,p,c} &= 9.68 - 10.00 = -0.32 \frac{kN}{m}
 \end{aligned}$$

Proofing Stresses for $q_{c,\uparrow}$

- Short-time strength for $20^\circ C$

$$\begin{aligned}
 n_{0,Ed} &= 1.35 \cdot n_{DL} + 1.00 \cdot n_p + 1.50 \cdot n_q \\
 &= 0 + 1.00 \cdot 20.00 + 1.50 \cdot 7.68 = 31.52 \frac{kN}{m} \stackrel{!}{<} perm.n_{0,Rd}
 \end{aligned}$$

- Short-time strength for $70^\circ C$

$$\begin{aligned}
 n_{\vartheta,Ed} &= 1.00 \cdot n_{DL} + 1.00 \cdot n_p + 1.50 \cdot n_q \\
 &= 0 + 1.00 \cdot 20.00 + 1.50 \cdot 7.68 = 31.52 \frac{kN}{m} \stackrel{!}{<} perm.n_{\vartheta,Rd}
 \end{aligned}$$

- Long-time strength for $20^{\circ}C$

$$\begin{aligned} n_{t,Ed} &= 1.35 \cdot n_{DL} + 1.50 \cdot n_p \\ &= 0 + 1.50 \cdot 20.00 = 30.00 \frac{kN}{m} \stackrel{!}{<} perm.n_{t,Rd} \end{aligned}$$

Comparison with RFEM

Determining the stresses for Member IV with the Finite Element Software *RFEM* gives following values:

- Stresses for $q_{c,\downarrow}$

$$n_{l,RFEM} = 20.31 \frac{kN}{m} \quad \rightarrow \text{Difference: } 1 - \frac{14.61}{20.31} = 28.1\%$$

$$n_{t,RFEM} = 12.22 \frac{kN}{m} \quad \rightarrow \text{Difference: } 1 - \frac{14.92}{12.22} = -22.1\%$$

- Stresses for $q_{c,\uparrow}$

$$n_{l,RFEM} = 19.95 \frac{kN}{m} \quad \rightarrow \text{Difference: } 1 - \frac{27.67}{19.95} = -38.7\%$$

$$n_{t,RFEM} = 8.97 \frac{kN}{m} \quad \rightarrow \text{Difference: } 1 - \frac{9.68}{8.97} = -7.9\%$$

10.3 Overview of the Stresses

Table 10-2 summarizes all maximal stresses for each member of the structure. It is clearly visible, that the choice of the membrane is mainly depending on Member I, Member II and Member IV, as there are the highest stresses.

Table 10-2: Overview of the stresses $\frac{kN}{m}$

	$perm.n_0$	$perm.n_\theta$	$perm.n_t$
Member I	26.42	26.42	21.00
Member II	29.56	29.56	24.00
Member III	14.09	14.09	9.00
Member IV	31.52	31.52	30.00

For the preliminary design, the maximal stresses of Member IV were taken into further account.

10.4 Required Tensile Strength of the Membrane

The required tensile strength will be calculated exemplary for both textile membranes and foils.

Textile Membrane

The design strength of textile membranes can be calculated, as is shown in Equation 6.6, with the help of several reduction factors A_i :

$$n_{t,d} = \frac{n_{t,c}}{\gamma_m \prod_0^3(A_i)}$$

- Short-time strength for 20°C: $perm.n_{0,d}$

$$\gamma_m = 1.2$$

$$A_0 = 1.2$$

$$A_1 = 1.6$$

$$A_2 = 1.2$$

$$A_3 = 1.1$$

$$\rightarrow n_{t,d} = perm.n_{0,c} \cdot \gamma_m \cdot \prod_0^3 = n_{t,c} \cdot 3.04$$

- Short-time strength for 70°C: $perm.n_{\vartheta,d}$

$$\gamma_m = 1.2$$

$$A_0 = 1.2$$

$$A_1 = 1.6$$

$$A_2 = 1.2$$

$$A_3 = 1.25$$

$$\rightarrow n_{t,d} = perm.n_{\vartheta,c} \cdot \gamma_m \cdot \prod_0^3 = n_{t,c} \cdot 3.456$$

- Long-time strength for 20°C: $perm.n_{t,d}$

$$\gamma_m = 1.2$$

$$A_0 = 1.2$$

$$A_1 = 1.7$$

$$A_2 = 1.2$$

$$A_3 = 1.1$$

$$\rightarrow n_{t,d} = perm.n_{t,Ed} \cdot \gamma_m \cdot \prod_0^3 = n_{t,c} \cdot 3.23$$

The final required tensile strength for textile membranes is the maximum value of each result above:

$$n_{t,d} = \max \begin{cases} perm.n_{0,c} \cdot 3.04 = 31.52 \cdot 3.04 = 95.82 \frac{kN}{m} \\ perm.n_{\vartheta,c} \cdot 3.456 = 31.52 \cdot 3.46 = 109.06 \frac{kN}{m} \\ perm.n_{t,c} \cdot 3.23 = 30.00 \cdot 3.23 = 96.90 \frac{kN}{m} \end{cases}$$

The required tensile strength of the structure build with textile membranes is $n_{t,c} = 119.06 \frac{kN}{m}$.

So, the chosen material is a PTFE-Glass-Fiber textile membrane with a strength of $115 \frac{kN}{m}$ in each main direction.

Foils

The design tensile strength of foils is described in Equation 6.7 and the help of reduction factors A_i , as well:

$$n_{t,d} = \frac{n_{t,c}}{\gamma_M \cdot \prod_{i=1}^3 (A_i)}$$

- Short-time strength for $20^\circ C$: $perm.n_{0,Rd}$

$$\gamma_m = 1.2$$

$$A_1 = 1.0$$

$$A_2 = 1.8$$

$$A_3 = 1.1$$

$$\rightarrow n_{t,d} = perm.n_{0,c} \cdot \gamma_m \cdot \prod_1^3 = n_{t,c} \cdot 2.38$$

- Short-time strength for $70^\circ C$: $perm.n_{\vartheta,Rd}$

$$\gamma_m = 1.2$$

$$A_1 = 1.0$$

$$A_2 = 1.6$$

$$A_3 = 1.1$$

$$\rightarrow n_{t,d} = perm.n_{\vartheta,c} \cdot \gamma_m \cdot \prod_1^3 = n_{t,c} \cdot 2.112$$

- Long-time strength for $20^\circ C$: $perm.n_{t,Rd}$

$$\gamma_m = 1.2$$

$$A_1 = 1.6$$

$$A_2 = 1.8$$

$$A_3 = 1.1$$

$$\rightarrow n_{t,d} = perm.n_{t,c} \cdot \gamma_m \cdot \prod_1^3 = n_{t,c} \cdot 3.802$$

Again, the final required tensile strength for foils is the maximum value of each result above:

$$n_{t,c} = \max \begin{cases} perm.n_{0,Ed} \cdot 2.38 = 31.52 \cdot 2.38 = 75.02 \frac{kN}{m} \\ perm.n_{\vartheta,Ed} \cdot 2.112 = 31.52 \cdot 2.11 = 66.19 \frac{kN}{m} \\ perm.n_{t,Ed} \cdot 3.802 = 30.00 \cdot 3.802 = 114.06 \frac{kN}{m} \end{cases}$$

The required tensile strength of the structure build with foils is $n_{t,d} = 114.06 \frac{kN}{m}$.

Manufacturing the structure with foils will be almost impossible, due to the high required tensile strength.

10.5 Discussion of the Results

Though the final results give a realistic setting, the difference between the results of the iteration process and the ones from the static software are partially enormous. This could be explained by overstepping one of the three requirements of Equations 9.19, 9.20 and 9.21 of the system in each member, the minimum ratio of height to length of 0.25. Especially the second direction, where the loading comes from below the system is subjected to this problem.

Member I

- Direction 1: $\frac{H}{L_1} = \frac{1.10}{3.60} = 0.30 > 0.25$ ✓
- Direction 2: $\frac{H}{L_2} = \frac{1.10}{10.80} = 0.10 < 0.25$ ×

Member II

- Direction 1: $\frac{H}{L_1} = \frac{1.10}{3.60} = 0.30 > 0.25$ ✓
- Direction 2: $\frac{H}{L_2} = \frac{1.10}{11.50} = 0.10 < 0.25$ ×

Member III

- Direction 1: $\frac{H}{L_1} = \frac{0.98}{3.60} = 0.27 > 0.25$ ✓
- Direction 2: $\frac{H}{L_2} = \frac{0.98}{6.30} = 0.16 < 0.25$ ×

Member IV

- Direction 1: $\frac{H}{L_1} = \frac{0.95}{2.20} = 0.43 > 0.25$ ✓
- Direction 2: $\frac{H}{L_2} = \frac{0.95}{10.80} = 0.09 < 0.25$ ×

Therefore, an exemplary calculation for Member I, with an alternated height of $3.00m$, which maintains the border of $\frac{H}{L} = \frac{3.00}{10.80} = 0.28 > 0.25$, was done to show the appropriateness of these rules.

The required pretensioning stresses decrease to:

$$n_{p,0,1} = 3.00 \frac{kN}{m}$$

$$n_{p,0,2} = 6.00 \frac{kN}{m}$$

The final stresses of the iteration process for the force $q_{c,\uparrow}$ were determined to:

$$n_{final,1} = 2.90 \frac{kN}{m}$$

$$n_{final,2} = 8.95 \frac{kN}{m}$$

In comparison the results of the finite element software for upward loadings are:

$$n_{RFEM,1} = 5.61 \frac{kN}{m}$$

$$n_{RFEM,2} = 5.73 \frac{kN}{m}$$

As can be easily seen, the results are now much more accurate, then the ones of the initial Member 1.

11 Conclusion and Prospect

The aim of this work, was to develop an universally usable tool to determine stresses of membrane structures for different loading cases and to summarize this newly obtained knowledge into an additional manual next to this current preparation.

Beside the main topic, this work also gives a short introduction to the general topic of membrane structures and describes their special properties and special components. The special safety concept for the membrane materials is given as well as some exemplary material characteristics. Another topic is the modeling of membrane surfaces for a static software, including the ex- and import and the utilization of those models. After the detailed explanation of the process of the determination of stresses inside the membrane system, an meticulous revised calculation of an exemplary membrane structure is shown.

One of the main issues for the determination of stresses of membrane structures is the direct correlation of shape of the structure and its ability to ablate loading.

Since it was only possible to determine the pretensioning stresses and their corresponding geometry of equilibrium with simple written calculations, it was an interesting task to develop a possible approach to extend those calculations to be also functioning for additional loading.

This was achieved by a literature research and the combination of several different approaches into an iteration process which determines a new geometry of equilibrium and its specific stresses in each step. This whole course of action was permanently monitored with the finite element software *RFEM* by *Dlubal*.

However, in this new approach, there are two topics, that has to be noted:

1. Though the iteration process determines the sags of each main direction anew in each step, they are non-real values and therefor only mathematical numbers. The actual shape is produces by the initial pretensioning stresses. Additional deformation is caused by elastic elongation of the membrane material due to the additional loading.
2. The boundaries and restrictions were determined by trial and error and the continuous monitoring and comparison with the finite element software.

One problematic issue was recognized in the application of the iteration process, specifically in the force dividing κ -approach, where the tensioning direction is subjected with increasing loading to decreasing divided loadings to the point that they are non-existent, where it should be the other way around. However, as this has not a major influence on the final results and the additional live loads are usually so small, that it can be neglected.

Further research could be done in the optimization of the iteration process, specifically as previously mentioned the κ -procedure. The development of geometry depending correction factors could be helpful, to improve the final determined stresses. Also the further examination of the restrictions and boundaries of this model would be important, to increase its safety and therefore its usefulness.

At last, as the following aphorism of George Edward Pelham Box says in other words, it is always important to know where the boundaries of a potential model are, to know in which areas it can be useful, but almost more important is to know when the results of a model are misleading and when it is more recommendable to search for another one.

"Essentially, all models are wrong, but some are useful."

- George Edward Pelham Box (1919 - 2013) -

Bibliography

- [1] Christian Satorius. Radnetz oder Trichternetz: Die Welt der Spinnennetze, 2015.
- [2] Baldachinnetz. Heckentiere — fabio rudolf, 2015.
- [3] Gerhard Rückert. *Wandelbare hybride Konstruktionen: Von der morphologischen Studie zum Prototyp*, volume 265 of *IBK-Bericht*. Birkhäuser, Basel u.a., 2001.
- [4] Rosemarie Wagner. *Bauen mit Seilen und Membranen*. Bauwerk. 2016.
- [5] Wisconsin History. Native American Tipis — Photograph — Wisconsin Historical Society, 2017.
- [6] Kopfball Redaktion. DasErste.de - Kopfball - Kopfball Bildergalerie, 01.01.2009.
- [7] Stadt Mannheim. Weiterer Umgang mit der Multihalle Mannheim — Mannheim.de, 2017.
- [8] Waiting for the Gig. HDR – Waiting for the GIG, 2012.
- [9] Seele. Allianz Arena, München, Deutschland - seele, 2016.
- [10] Christoph Gengnagel. *Mobile Membrankonstruktionen*. Dissertation, Technische Universität München, München, 2005.
- [11] Kunststoffrohrverband e.V. Kesselformel, 2017.
- [12] Werner Sobek Group. Drehende Schirme — Werner Sobek, 2003.
- [13] Dlubal Software GmbH. RF-FORM-FINDING: Form-Finding of Membrane and Cable Structures, 2016.
- [14] Michael Seidel. *Tensile surface structures: A practical guide to cable and membrane construction ; materials, design, assembly and erection*. Ernst, Berlin, 2009.
- [15] TU Dortmund. Bauelemente von Drahtseilen.
- [16] Zeno. Drahtseile, 2017.
- [17] Atelier Frei Otto Warmbronn. Frei Otto_Bundesgartenschau 1955_01_Musikpavillon_Kassel 1955_Foto Atelier Frei Otto Warmbronn — BDA — der architekt, 1995.
- [18] sinoramabus. The Olympic Stadium of Montreal, 2010.
- [19] NetCompositesNow. Woven Fabrics.
- [20] Deutsches Institut für Normung. DIN 4134:1983-02 Tragluftbauten; Berechnung, Ausführung und Betrieb.
- [21] Jan Knippers. *Atlas Kunststoffe + Membranen: Werkstoffe und Halbzeuge, Formfindung und Konstruktion*. Edition Detail. Inst. f. Internat. Arch.-Dok, München, 1. Aufl. edition, 2010.

- [22] mb AEC. *Bemessungs- und Konstruktionshilfen für Stahlbauwerke nach Eurocode 3: (DIN EN 1993-1-1:2010-12 und DIN EN 1993-1-1/NA:2010-12)*.
- [23] Prof.-Dr.-Ing.-Robert Pawlowski. Tragwerksentwurf - Membranen und Seilnetze. 2016.
- [24] Prof. Dr. sc. techn. Mike Schlaich, Dr.-Ing Anette Bögle, and Dipl.-Ing. Achim Bleicher. Brückenbau II - Seile. 2011.
- [25] Reinhard Wendehorst. *Wendehorst Bautechnische Zahlentafeln*. Vieweg & Teubner, Wiesbaden, 34., vollst. überarb. u. erw. Aufl. edition, 2012.